

UNCLASSIFIED

AD. 297 289

*Reproduced
by the*

**ARMED SERVICES TECHNICAL INFORMATION AGENCY
ARLINGTON HALL STATION
ARLINGTON 12, VIRGINIA**



UNCLASSIFIED

NOTICE: When government or other drawings, specifications or other data are used for any purpose other than in connection with a definitely related government procurement operation, the U. S. Government thereby incurs no responsibility, nor any obligation whatsoever; and the fact that the Government may have formulated, furnished, or in any way supplied the said drawings, specifications, or other data is not to be regarded by implication or otherwise as in any manner licensing the holder or any other person or corporation, or conveying any rights or permission to manufacture, use or sell any patented invention that may in any way be related thereto.

63-2-5

RADC-TR-61-217

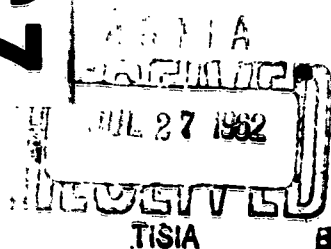
297289

UNIVERSITY
OF ALASKA

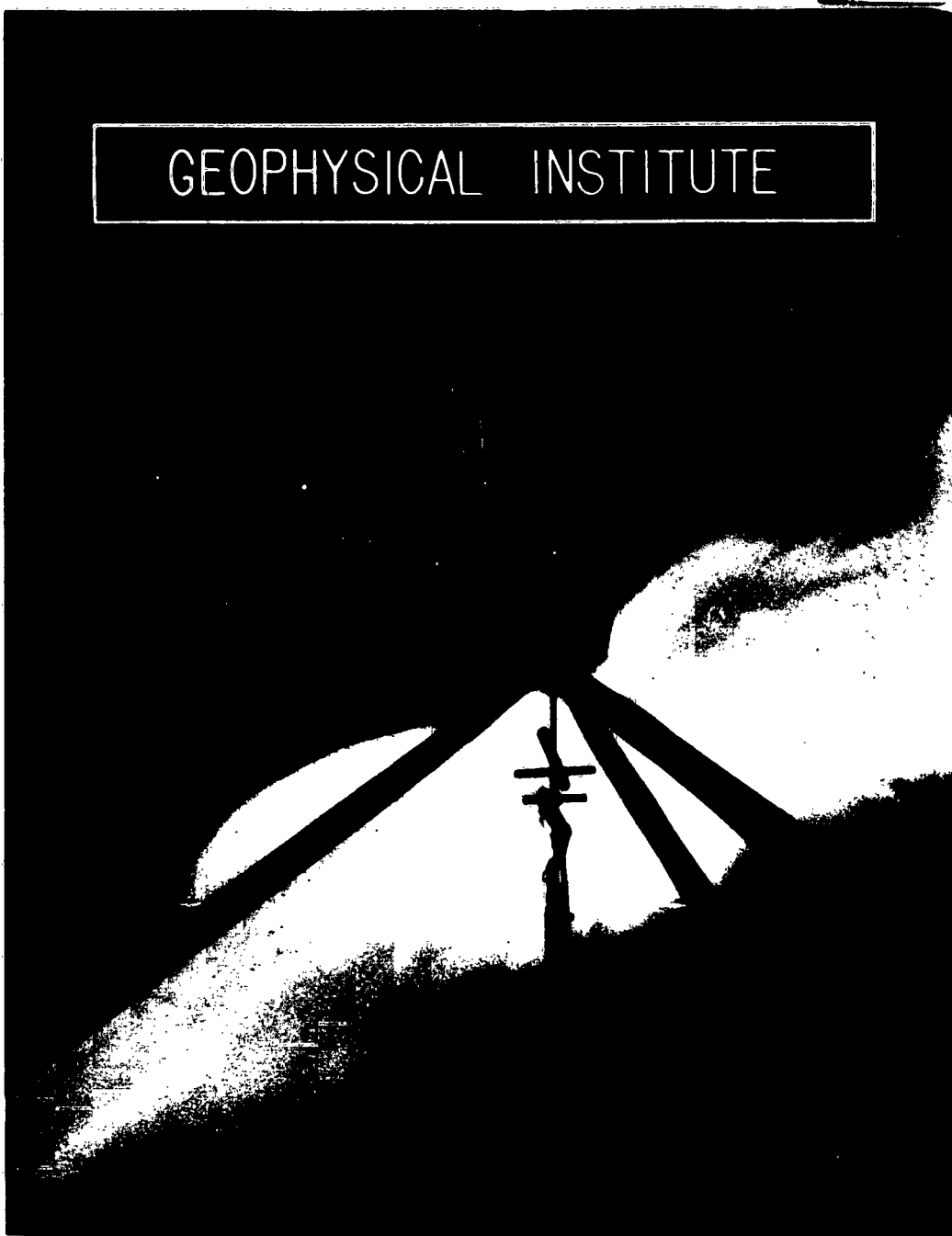
COLLEGE
ALASKA

CATALOGED BY ASTIA
AS AD NO.

297 289



GEOPHYSICAL INSTITUTE



RADIO PROPERTIES OF THE AURORAL IONOSPHERE - PART 3

Final Report

March 1962

Air Force Contract No. AF 30(635)-2887
Project No. 5535 - Task 45774

Rome Air Development Center
Griffiss Air Force Base
Rome, New York

TABLE OF CONTENTS - PART 3

| | Page |
|-----------------------|------|
| List of Illustrations | 1 |
| List of Tables | 11 |

III Observations of Radio Star Scintillations During Aurora by Robert F. Benson

| | |
|-----------------|---|
| 1. Introduction | 1 |
| 2. Observations | 2 |
| 3. Conclusions | 5 |
| References | 6 |

IV Radio Star Scintillations and Spread F by Z. A. Ansari

| | |
|-----------------------|----|
| 1. Introduction | 11 |
| 2. Method of Analysis | 12 |
| References | 14 |

V Scintillation of Satellite Radio Signals in the Auroral Zone by Roy P. Basler and Ronald N. DeWitt

| | |
|---|----|
| 1. Introduction | 16 |
| 2. Direct Measurement of Heights | 16 |
| 3. A Method for Determining the Height Distribution of the Irregularities | 19 |
| 3.1 Diurnal and seasonal variations | 21 |
| 3.2 Variation of scintillation with geomagnetic activity | 21 |
| 3.3 Variation of scintillation with satellite altitude | 22 |
| 4. Discussion | 25 |
| References | 26 |

VI Satellite Radio Signal Determinations of Upper F Region Electron Densities in the Auroral Zone

by

W. B. Murcray and J. H. Pope

| | |
|--|----|
| Text | 30 |
| Appendix - Doppler Shifts in Ionized Media | 38 |
| References | 41 |

VII Observations of High Latitude Radio Aurora

by

Leif Owren

| | |
|--|----|
| 1. Introduction | 45 |
| 2. Visual Aurora in High Latitudes | 46 |
| 3. Radio Aurora in High Latitudes | 47 |
| 4. Theory of Scattering in Field-Aligned Irregularities | 50 |
| 5. High Latitude Observations of Radio Aurora | 54 |
| 6. Summary and Discussion of College Observations Between 12-800 Mc/s | 56 |
| 6.1 Diurnal variation | 56 |
| 6.2 Range distribution | 57 |
| 6.3 Azimuth distribution | 58 |
| 6.4 Longitudinal correlation distance | 58 |
| 7. Auroral Fading Rates | 59 |
| 8. Auroral Doppler Shifts | 59 |
| 9. The Radio Auroral Zone | 61 |
| Appendix - Distortion of the Magnetic Field | 62 |
| - Refraction and Auroral E Layer Electron Densities | 63 |
| - Volume Scattering | 64 |
| References | 66 |
| APPENDIX I - Contents of Previous Reports | 73 |

List of IllustrationsPage

| | | |
|------------|--|----|
| Fig. III.1 | Long-duration fade and heavy scintillation on the 223 Mc phase-switch record between 2058 and 2107 150° WMT on November 26, 1959 | 7 |
| Fig. III.2 | All-sky camera photographs from 2044-2113 150° WMT on 26 November 1959. The radio source in Cassiopeia is indicated by the white circle near the center in each photograph. Geomagnetic north is to the right | 8 |
| Fig. III.3 | All-sky camera photographs from 2105-2116 150° WMT on November 30, 1959. The radio source in Cassiopeia is indicated by the white circle near the center in each photograph. Geomagnetic north is to the right | 9 |
| Fig. III.4 | Phase-switch records for November 30, 1959. Time indicated is 150° WMT | 10 |
| | * * * * * | |
| Fig. IV.1 | Radio Star Scintillations and Spread F at College | 15 |
| | * * * * * | |
| Fig. V.1 | Example of spaced receiver recordings from which a height measurement was made. These recordings were made on December 12, 1959, and the height measured in this case was 430-460 km | 27 |
| Fig. V.2 | Signal strength recording showing examples of all three scintillation indices. The recording was made on June 26, 1958 | 27 |
| Fig. V.3 | Diurnal variation of scintillation indices 0, 1, and 2 | 28 |
| Fig. V.4 | Seasonal variation of scintillation indices 0, 1, and 2 | 28 |
| Fig. V.5 | Variation of scintillation indices 0, 1, and 2 with College K-index | 29 |
| Fig. V.6 | Dependence of scintillation indices 0, 1, and 2 on satellite altitude. The straight lines represent the idealized dependence which would be observed if irregularities occurred with equal probability below 650 km and were absent at greater heights | 29 |

| <u>List of Illustrations (Con't)</u> | <u>Page</u> |
|---|-------------|
| Fig. VI.1 Electron densities over Alaska 4 Nov 1957 (150°WMT) | 42 |
| Fig. VI.2 Geometry of satellite pass 4 Nov 1957 1010 (150°WMT) | 43 |
| Fig. VI.3 Electron densities over Alaska 8 Nov 1957 (150°WMT) | 44 |
| Fig. VI.4 Electron densities over Alaska 6 Nov 1957 (150°WMT) | 44 |
| * * * * * | |
| Fig. VII.1 The pattern of auroral alignment and motion deduced for the northern hemisphere and showing the position of 13 high-latitude stations relative to the pattern at 4 universal times. The stations are College (C), Alert (A), Thule (T), Resolute Bay (R), Godhavn (G), Baker Lake (BL), Churchill (CH), Meanook (M), Saskatoon (S), Kiruna (K), Barrow (B), Cape Chelyuskin (CC), and Cape Schmidt (CS). The fixed coordinate system indicates geographic co- latitude and local time, and the mobile one indicates geomagnetic colatitude and longitude. Heavy lines represent the aurora, and arrowheads on the lines indicate the direction of motion of irregularities along the auroral forms. The straight, dashed line near midnight separates the regions of primarily westward and primarily eastward auroral motion at the auroral zone (After Davis, 1961) | 68 |
| Fig. VII.2 | 69 |
| Fig. VII.3 | 69 |
| Fig. VII.4 | 70 |
| Fig. VII.5 | 70 |
| Fig. VII.6 | 71 |
| Fig. VII.7 | 71 |
| Fig. VII.8 Regions from which Doppler shifted auroral echoes were obtained by Nichols (lightly shaded areas) and by Leadebrand et al (solid black area) relative to the auroral pattern deduced by Davis at times (a) prior to magnetic midnight, (b) near magnetic midnight, and (c) after magnetic midnight | 72 |

List of Tables

Page

Table V.I

19

Table V.II

22

Table V.III

24

* * * * *

III OBSERVATIONS OF RADIO STAR SCINTILLATIONS DURING AURORA

by

Robert F. Benson

1. Introduction

In the course of an investigation of radio star scintillations in England, Little and Maxwell¹ found the scintillations to be enhanced during intense auroral activity but to be unaffected by a stable auroral arc slowly moving across the line-of-sight to the radio star. The observations at the Geophysical Institute of the University of Alaska, located within the auroral zone, show a significant correlation between radio star scintillation amplitude at 223 Mc and the occurrence of aurora^{2,3}. The experimental evidence indicates that aurora is always accompanied by radio star scintillation whereas the converse is not true. These results were obtained from a statistical analysis, both on a daily basis and on an hourly basis, of scintillation and all-sky camera auroral data for the winter of 1957-58 and for September 1958. On the basis of these results, it seemed profitable to look more closely at individual recordings showing unusual scintillation or auroral activity. This section presents some preliminary results of this study.

Auroral data were obtained from the all-sky camera at College. This camera photographs the entire sky, with the exception of a small region in the zenith, once a minute on Kodak tri-x film using a 15 second exposure. Elevation is indicated by small lights every 10° in the geomagnetic E-W direction and every 30°

in the geomagnetic N-S direction (Fig. III.2).

2. Observations

During November and December of 1959 the radio source in Cassiopeia was tracked continuously with the 223 Mc phase-switch interferometer in an effort to determine the effect of aurora in the line-of-sight on the scintillations of the radio star signal. A minute to minute correlation was sought between the all-sky camera records and the observed star scintillations. Several cases were found where auroral forms apparently had a direct effect on scintillation activity. This effect was most pronounced if the level of scintillation activity was low before the auroral form crossed the star position.

During the period of observation, the radio star was high in the southern sky and near the geomagnetic zenith (13° south of the geographic zenith at College). The auroral forms crossing the line-of-sight were very active, as is often the case with aurora near the zenith at College.

Two nights, November 26 and 30 were of special interest. On 26 November, during an active auroral display, a long-duration fade of the radio star signal was observed on the 223 Mc phase-switch interferometer. Long-duration fades have been observed previously at College, and have been discussed extensively elsewhere^{3,4}. They are characterized by an almost complete disappearance of the sinusoidal trace produced by the radio star on the phase-switch interferometer record, and may last for as long as an hour in extreme cases. Their cause has been attributed to the occurrence of angular deviations greater than

the lobe-width of the interferometer pattern, coupled with the irregularities becoming smaller in angular size than the source (Cassiopeia, angular diameter $4'$).

Fig. III.1 shows the long-duration fade as seen on the 223 Mc phase-switch record. Between 2058 and 2107 the characteristic sinusoidal trace can be seen to disappear coinciding with a period of intense scintillation. Auroral activity began at 2039 on this night, and individual all-sky camera frames from 2044 through 2113 are presented in Fig. III.2. A great increase in the scintillation activity is observed as the rapidly moving aurora crosses the star position, which is indicated by the white circle slightly to the left of center on each frame. The auroral activity shown in Fig. III.2 can be summarized as follows:

- 2044-2057 active auroral form - occasionally passing through star position
- 2058-2059 intense band through star position
- 2100-2101 slight breakup and swirl of activity
- 2102-2107 high point of band is very stable and passes through star position
- 2108-2109 band moves to the south of the star position
- 2110-2113 aurora remains south of star position

The shift in the band away from the star position coincides exactly with the recovery of the sinusoidal trace in the interferometer record.

An investigation of the riometer⁵ data, which is a continuous presentation of the intensity of 27.6 Mc galactic radio waves, indicated that no noticeable increase in the absorption

at 27.6 Mc was present during the long-duration fade. The radio meter uses an antenna with a beamwidth of about 60° by 100° and thus measures the integrated absorption over a large area of the sky. This could explain the lack of absorption associated with the narrow auroral band during the above event.

All-sky camera records corresponding to the times of previous observations of long-duration fades were examined, but no conclusions could be reached because of poor records caused by cloudy conditions or instrumentation difficulties.

On 30 November, both aurora and radio star scintillations were present intermittently during most of the night. One active auroral sequence is presented in Fig. III.3, and the corresponding section of the phase-switch interferometer record is presented in Fig. III.4. The aurora at 2112 shows a definite change in shape from the previous forms and is beginning to cross the star position. On frames 2113, 2114, 2115, and 2116 the aurora is extremely intense and is directly in the line of sight to the radio star. Corresponding to this transition in the aurora at 2112, there was an onset of heavy scintillation activity marked by an extremely deep scintillation. This scintillation occurred at the 'zero crossing' of the sinusoidal trace, when the signals at the two antennas of the interferometer were in phase quadrature. At these zero crossings the sensitivity of the phase-switch interferometer drops to zero, so that this particular scintillation can best be interpreted as an 'angular scintillation' i.e., a temporary deviation of the apparent position of the star by approximately one-quarter of

the interferometer lobe-width (about 10 minutes of arc for the antenna spacing of 100 yards). Also starting at 2112, the riometer indicated a sudden 4 db increase in the absorption at 27.6 Mc indicating the appearance of large amounts of ionization at low levels in the ionosphere. The absorption reached a maximum of 10 db at 2125.

During both of the above nights, as well as the other nights studied, there were cases when intense rapidly moving auroral forms crossed the star position with no noticeable effect on the scintillation activity. These were usually periods in which high scintillation activity was present before the aurora appeared, or before the aurora crossed the star position, so that the effect of the aurora, if any, was difficult to identify.

3. Conclusions

The data presented for 26 and 30 November show clearly that the presence of aurora in the line-of-sight to the radio star can directly affect the observed scintillations of the radio signal. The observations do not imply that the irregularities giving rise to the scintillations were located at the same level as the most intense portion of the visual aurora which was probably located in the neighborhood of 100 km. It is emphasized that the all-sky camera and interferometer records for the two special events reproduced in this section indicate that the onset of the line-of-sight aurora and the onset of the extreme changes in the scintillation records were separated by at most one minute.

References

- 1 Little, C. G., and A. Maxwell, Scintillation of radio stars during aurorae and magnetic storms, J. Atmospheric and Terrest. Phys., 2, 356-360, 1952.
- 2 Reid, G. C., and E. Stiltner, Radio properties of the auroral ionosphere, Quart. Progr. Rept. 13, Air Force Contract AF 30(635)-2887, Project 5535 - Task 45774, Geophys. Inst. Rept. No. UAG-R94, College, Alaska, 1959.
- 3 Little, C. G., G. C. Reid, and E. Stiltner (in preparation).
- 4 Little, C. G., R. P. Merritt, E. Stiltner, R. Cognard, Radio properties of the auroral ionosphere, Quart. Progr. Rept. 6, Air Force Contract AF 30(635)-2887, Project 5535 Task 45774, Geophys. Inst. Rept. No. UAG-R70, College, Alaska, 1957.
- 5 Little, C. G., and H. Leinbach, The riometer - a device for the continuous measurement of ionospheric absorption, Proc. IRE, 47, 315-320, 1959.

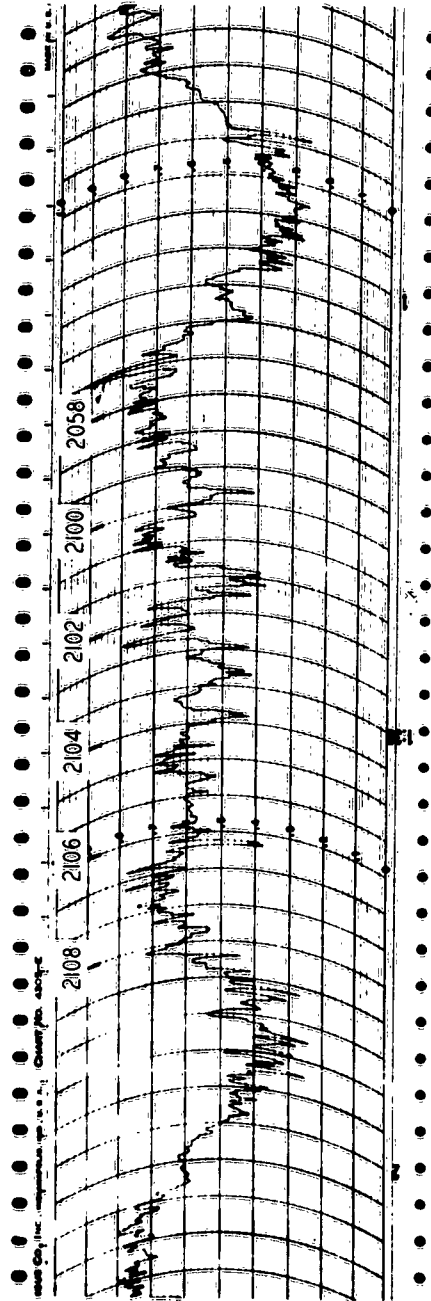


Fig. III.1 Long-duration fade and heavy scintillation on the 223-Mc phase-switch record between 2058 and 2107 150° WMT on November 26, 1959.

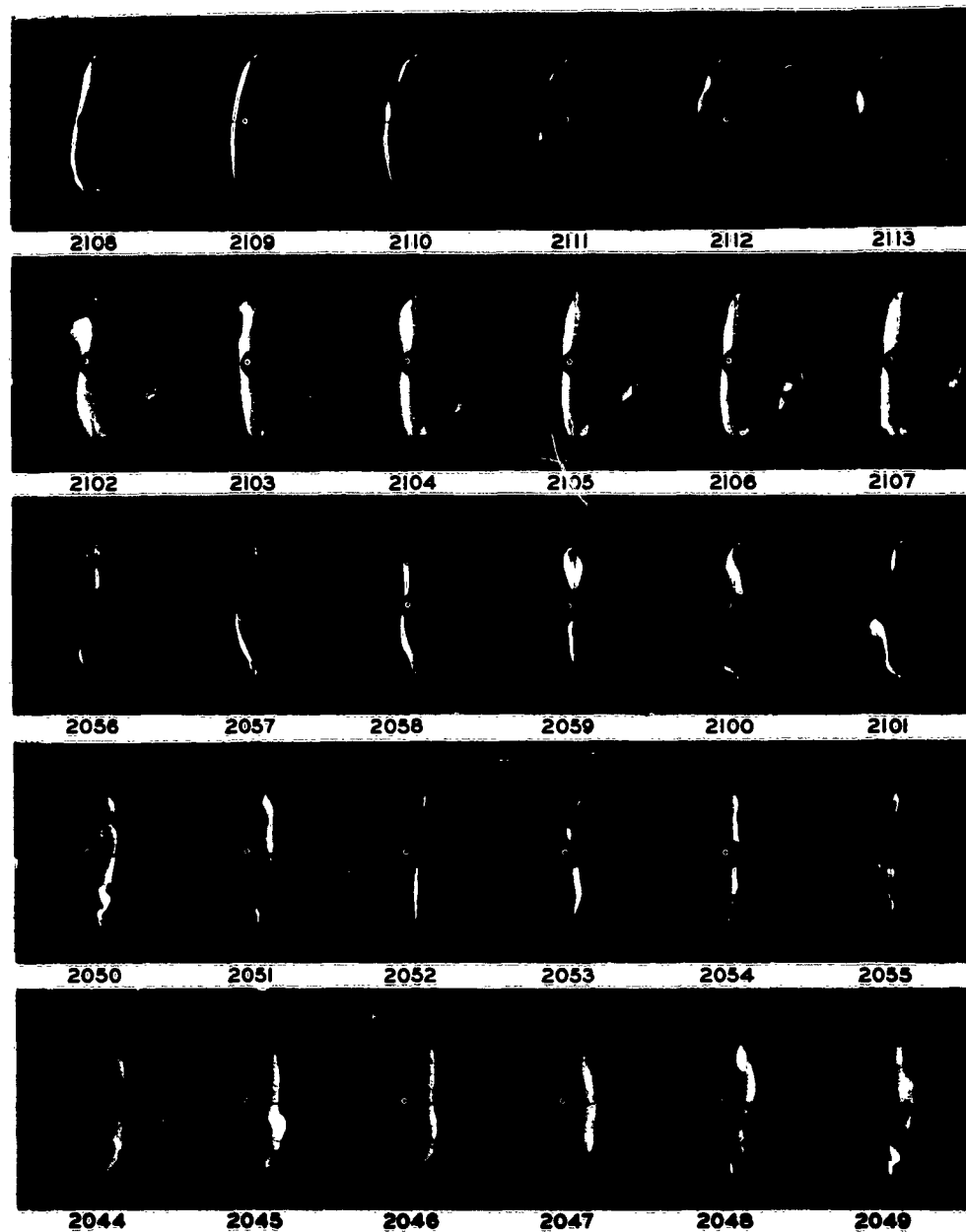


Fig. III.2 All-sky camera photographs from 2044-2113 150° WMT on 26 November 1959. The radio source in Cassiopeia is indicated by the white circle near the center in each photograph. Geomagnetic north is to the right.

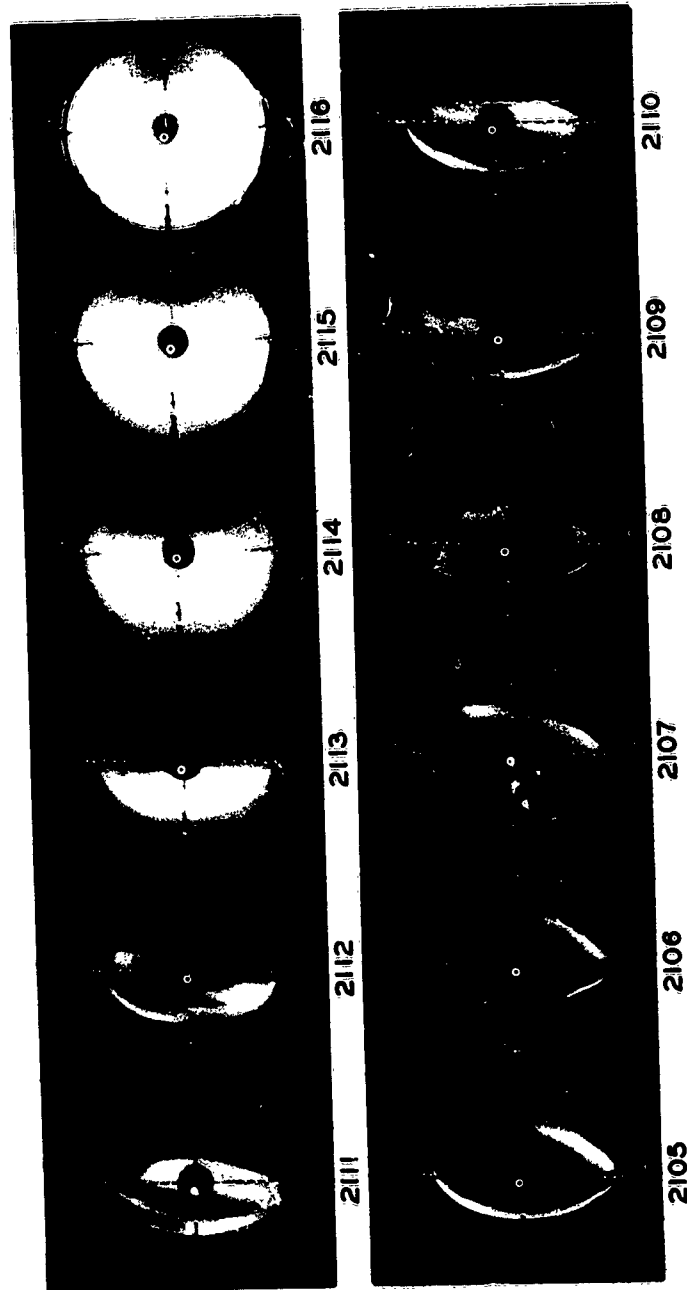


Fig. III.3 All-sky camera photographs from 2105-2116 150° WMT on November 30, 1959. The radio source in Cassiopeia is indicated by the white circle near the center in each photograph. Geomagnetic north is to the right.

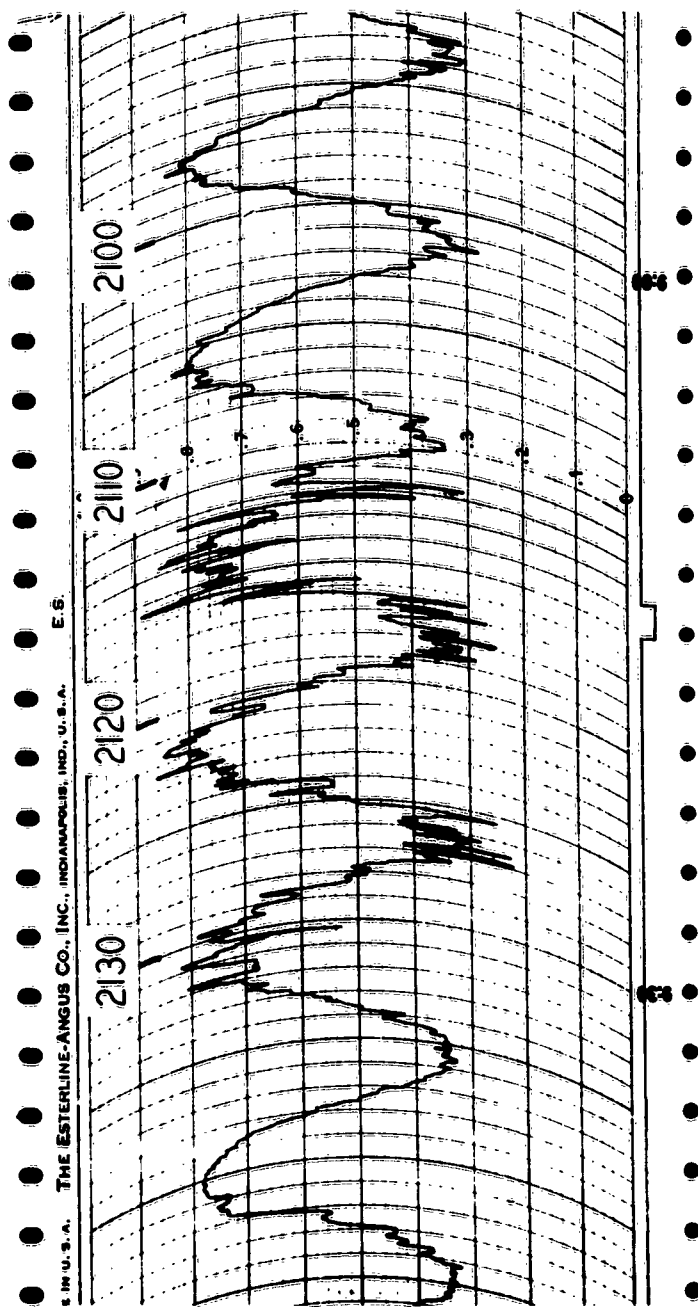


Fig. III.4 Phase-switch records for November 30, 1959.
Time indicated is 150° UT.

IV RADIO STAR SCINTILLATIONS AND SPREAD F

by

Z. A. Ansari

1. Introduction

It is generally believed that radio star scintillations and spread F are caused by some sort of scattering mechanism from the irregularities of the ion density. The former is essentially a forward scattering phenomenon while the latter is probably a combination of both forward and back scattering. It is quite possible that the irregularities of ion density responsible for spread F may be different from those which are responsible for radio star scintillations but with the present state of our knowledge it is generally thought desirable to assume a common origin of the irregularities¹. At Cambridge, Ryle and Hewish², and at Manchester, Little and Maxwell³, a high correlation was found between radio star scintillation and spread F but in Australia, Bolton, Slee and Stanley⁴ observing at low angles of elevation did not find any correlation between amplitude scintillations and spread F. A partial correlation was found, however, by Mills and Thomas⁵ in Australia between fluctuation index and a measure of F-region activity, which in part includes spread F activity also. Hartz in Canada after making a simultaneous study of radio star scintillations and Spread F at Ottawa found no definite correlation between the two. He found a considerable angle of elevation dependence in the data i.e. at low angles of elevation scintillations occurred more frequently.

2. Method of Analysis

The actual procedure of estimating spread F by visual inspection was given up in favor of a more quantitative method based on the actual amount of spread in Mc/s measured from the ionograms. It may be pointed out here that at high latitudes this method is most suitable owing to the fact that the ionograms show very well defined inner and outer edges and hence the amount of spread can be measured accurately.

A fine spread F index scale from 0 to 9 was used. Spread F index was taken to be proportional to the total spread which is defined as Follows:

Total spread = spread in the ordinary branch + spread in extraordinary branch.

The description of the scale is as follows:

| Spread F index is | When | Total spread is between |
|----------------------|------|----------------------------|
| 0 | | 0 Mc/s - .2 Mc/s |
| 1 | | .3 " - .7 " |
| 2 | | .8 " - 1.2 " |
| 3 | | 1.3 " - 1.7 " |
| 4 | | 1.8 " - 2.2 " |
| 5 | | 2.3 " - 2.7 " |
| 6 | | 2.8 " - 3.2 " |
| 7 | | 3.3 " - 3.7 " |
| 8 | | 3.8 " - 4.2 " |
| 9 | | > 4.3 " |

Radio-star scintillation data taken at College, Alaska at 223 and 456 Mc/s was available for April through September 1958. The

data was not continuous as each one of the sources Cygnus or Cassiopeia was tracked continuously for four days and then the other source started. Amplitude scintillations indices obtained by visual inspection of scintillations records were available for comparison with spread F indices. Result of the comparison is showed in Fig. IV.1. It appears as if no definite correlation between the two phenomenon exists.

References

- 1 Booker, H. G., "The use of Radio Stars to study Irregular Refraction in the Ionosphere", Proc. IRE, 46, 298-313, 1958.
- 2 Ryle, M. and A. Hewish, "The Effects of the Terrestrial Ionosphere on the Radio Waves from Discrete Sources in the Galaxy", Monthly Notices Royal Astronomical Society, 110, pp. 384-394, 1950.
- 3 Little, C. G. and A. Maxwell, "Fluctuation in the Intensity of Radio Waves from Galactic Sources", Phil Mag., 42, 267-278, 1951.
- 4 Bolton, J. G., O. B. Slee, and G. J. Stanley, "Galactic Radiation at Radio Frequencies IV. Low Altitude Scintillation of the Discrete Sources", Aust. Jour. Phys., A6, 434-451, 1953.
- 5 Mills, B. Y. and A. B. Thomas, "Observations of the Source of Radio Frequencies Radiated in the Constellation of Cygnus", Aust. Jour. Phys., A4, 158-171, 1951.

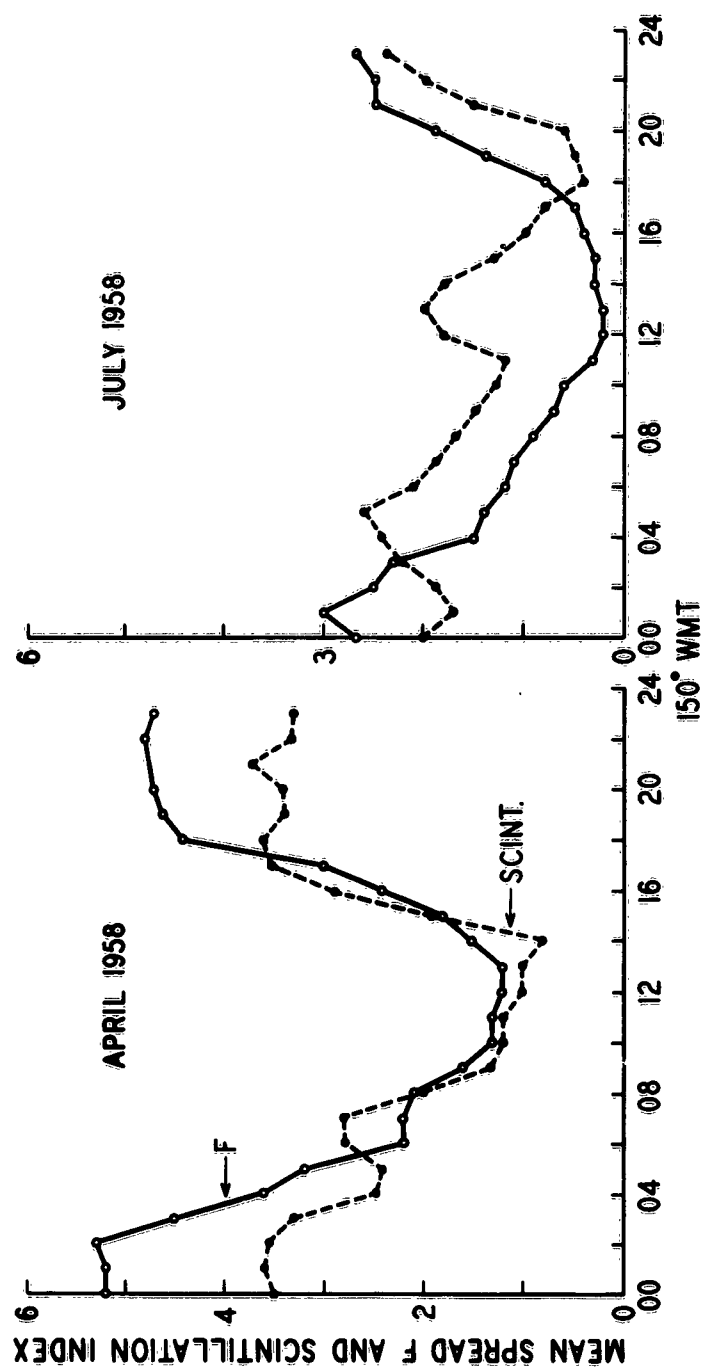


Fig. IV.1 Radio Star Scintillations and Spread F at College.

V SCINTILLATION OF SATELLITE RADIO SIGNALS IN THE AURORAL ZONE

by

Roy P. Basler and Ronald N. DeWitt

1. Introduction

The presence of electron density irregularities in the ionosphere has been well established by observations of scintillations of radio stars, but the height at which these irregularities occur has been a subject of some controversy¹. As a new approach to this subject, studies based on satellite radio transmissions have been made in several different parts of the world. In Australia, Slee² concluded that the irregularities must lie below 350 km. From observations made in England, Kent³ placed their height above 250 km and decided they were probably most concentrated between 270 and 320 km. In Illinois, Yeh and Swenson⁴ observed scintillations which they concluded were produced by irregularities lying between 200 and 300 km.

Evidence is presented which suggests that the inhomogeneities responsible for the violent fluctuations in the satellite radio signal strength recorded in College, Alaska, are distributed from 145 to 1000 km although they are relatively scarce above 600 or 700 km.

2. Direct Measurement of Heights

The 65° latitude of College was very nearly equal to the orbital inclination of the satellite 1958δ₂, so when the satellite passed overhead at College it traveled in a west-east direction. On the ground, the diffraction pattern caused by

ionospheric irregularities moved in an east-west direction with a velocity determined by the ratio of the satellite's height to the height of the irregularities. Thus, if the ground velocity of the diffraction pattern could be determined, and if the satellite's height and velocity were known, the height of the irregularities could be measured directly by simple geometry⁵. A small error was introduced by ionospheric refraction, but correction for this did not seem warranted in view of the limited accuracy of the measurements.

The measurements were made using two receiving stations separated by 19 km on an east-west line. Each station employed a circularly polarized "turnstile" antenna to reduce the effects of Faraday rotation while the satellite was near overhead. The satellite's 20 Mc/s signal strength was observed by recording the AGC voltages of Collins 51J-4 receivers on Sanborn recorders with chart speeds of either 5 or 10 mm/sec. Since the recording stations were independent, a means for supplying synchronous time marks was necessary. This was provided by a narrow band frequency modulated radio link that actuated the time-mark system at each location. To simplify the operation of the remote station, a radio operated control system was devised which was also actuated by tones carried by the time-mark radio link.

The choice of a relatively large separation between receiving stations precluded the possibility of using the fine detail of the diffraction pattern for height determinations, so height measurements could only be made when some gross feature of the pattern could be identified on both recordings. Typically,

this feature was a sudden onset of scintillation, or in some cases, an abrupt increase in the rate or amplitude of the fluctuation. A typical example of records from which one of these measurements was made is shown in Fig. V.1.

The time difference between the appearance of a feature at the west and the east station was measured, and the height of the irregularities was computed using the relation

$$\frac{vT}{L} = \frac{H - h}{h}$$

where H is the height of the satellite, h is the height of the irregularities, L is the distance between receiving stations, v is the satellite's velocity, and T is the time taken by a feature of the diffraction pattern in traversing the distance L . The height and velocity of the satellite were determined from information supplied by the Smithsonian Astrophysical Observatory's Satellite Tracking Program.

The results of these measurements are given in Table V.I. The two heights listed in each instance indicate the limits imposed by the possible error in the measurement of T , the difference in time of occurrence at the two stations. The heights measured fall in the range from 145 to 1000 km, suggesting that no single height can be associated with the scintillation producing regions. Heights are obtained only from irregularities producing a recognizable feature in the diffraction pattern as observed at the two stations. The values, therefore, should not be interpreted as exclusive heights for the irregularities during the satellite passes, since other irregularities capable of

producing scintillations could simultaneously exist at other heights. For example, on December 18, 1959, irregularities were observed at both 290 and 460 km during a single recording. It should also be pointed out that these measurements refer only to a small portion of the boundary of the regions containing the irregularities. Thus, the values given might in some cases be the upper or lower limits of regions having a considerable vertical extent.

TABLE V.I

| <u>Date</u> <u>1959</u> | <u>Universal</u> <u>Time</u> | <u>Height</u> <u>km</u> | <u>Date</u> <u>1959</u> | <u>Universal</u> <u>Time</u> | <u>Height</u> <u>km</u> |
|----------------------------|---------------------------------|----------------------------|----------------------------|---------------------------------|----------------------------|
| June 10 | 0243 | 850-1150 | Oct. 2 | 1720 | 360-520 |
| June 11 | 2309 | 670-830 | Oct. 8 | 1838 | 240-270 |
| June 12 | 2356 | 570-670 | Nov. 25 | 0325 | 500-680 |
| June 13 | 0138 | 390-440 | Nov. 26 | 0316 | 350-420 |
| June 24 | 2105 | 510-610 | Dec. 4 | 0004 | 300-360 |
| Aug. 15 | 0607 | 300-340 | Dec. 12 | 2140 | 430-460 |
| Sept. 9 | 0223 | 680-930 | Dec. 18 | 1940 | 260-320 |
| Sept. 19 | 2330 | 310-400 | Dec. 18 | 2254 | 380-540 |
| Sept. 19 | 2153 | 170-180 | Dec. 18 | 2256 | 140-150 |
| Sept. 22 | 1930 | 420-1040 | Dec. 25 | 1832 | 430-600 |
| Sept. 22 | 1931 | 190-210 | Dec. 25 | 2010 | 200-280 |
| Sept. 22 | 2250 | 230-280 | | | |

3. A Method for Determining the Height Distribution of the Irregularities

There was no way of controlling the sampling for the spaced receiver measurements, and no statistical weight could be given to

the heights listed in Table V.I. Therefore, the following method was employed to determine whether or not there was any preferred height of irregularity occurrence.

The perigee precession of 1958 δ_2 caused the heights of the passages over Alaska to vary from 200 to 1250 km during the satellite's lifetime of nearly two years. The variation of the occurrence of scintillation in the signal received from these different heights should indicate the vertical distribution of the irregularities responsible for the scintillation. This is because there was greater probability that the satellite would be eclipsed by irregularities when its height was increased in the range through which irregularities could occur.

The method was very similar to that used by Yeh and Swenson⁴. The amount of fluctuation of signal strength was classified subjectively according to the following arbitrary scintillation indices:

| <u>Index</u> | <u>Character of Signal</u> |
|--------------|--|
| 0 | No scintillation. No deviation from smooth Faraday fading pattern. |
| 1 | Slight scintillation but Faraday pattern still discernable. |
| 2 | Strong and rapid scintillation sufficient to completely obscure Faraday pattern. |

Frequently an entire record could be classified by one index, but more common were the instances when a record would be divided between two or three indices. An example of all three indices occurring in a short section of one record is shown in Fig. V.2.

3.1 Diurnal and seasonal variations

The total time for each recording was divided on a percentage basis between the three indices. These percentages were averaged according to the month of the satellite passage and the hour of closest approach. The results are given in Figs. V.3 and V.4.

Figs. V.3 and V.4 demonstrate nighttime and winter maximums of scintillation similar to those which have been indicated by radio star observations at College⁶. This is also the general behavior reported by Yeh and Swenson⁴ for their satellite observations. It should be pointed out that these histograms only indicate the general form of the diurnal and seasonal variations since the sampling in some intervals was not sufficiently large to average out the effects of other possible parameters such as the height of the satellite, magnetic activity, and solar zenith angle.

Index 1 seems to vary about an average value of approximately 40 per cent and has no apparent temporal dependence.

3.2 Variation of scintillation with geomagnetic activity

College K-Index was tabulated for each recording as a convenient index of local geomagnetic activity, and the total time for each recording was divided on a percentage basis between the three scintillation indices. These percentages were averaged for each value of College K-Index. The results are shown in Fig. V.5, and the number of samples for each value of College K-Index are given in Table V.II.

TABLE V.II

| <u>College K-Index</u> | <u>Number of Samples</u> | <u>College K-Index</u> | <u>Number of Samples</u> | <u>College K-Index</u> | <u>Number of Samples</u> |
|----------------------------|------------------------------|----------------------------|------------------------------|----------------------------|------------------------------|
| 0 | 12 | 3 | 95 | 6 | 7 |
| 1 | 85 | 4 | 47 | 7 | 7 |
| 2 | 121 | 5 | 42 | 8 | 1 |

Fig. V.5 shows an increase of scintillation with increasing geomagnetic activity, which is the same general relation observed at lower latitudes for radio star scintillation⁷.

3.3 Variation of scintillation with satellite altitude

The recordings average about five minutes in length although they vary from one to ten minutes. When the satellite was near perigee its height changed as much as 200 km during a recording. The range from 200 to 1250 km was divided into 50 km intervals and for each pass through one of these intervals the time distribution, in per cent, over the three indices was recorded. These percentages were then averaged for each interval. The heights were computed from information supplied by the Space Track Control Center and by the Smithsonian Astrophysical Observatory's Satellite Tracking Program.

The results of this analysis are plotted in Fig. V.6. As before, the values for index 1 vary randomly about an average value of approximately 40 per cent and so apparently have no height dependence.

The straight lines drawn in Fig. V.6 represent the height

dependence which would be expected if the regions containing the irregularities occurred with equal probability at all heights up to 650 km and were absent at greater heights. This is an overly simplified model for ionospheric structure, but it is a useful first approximation for explaining the apparent trend of the data. Considering the four examples listed in Table V.I for which the height was considerably above 650 km, it seems that instead of going to zero above this height, the number of irregularities decreases to a small but finite fraction of the total number at lower altitudes.

At the extreme high and low altitudes there are large deviations from the overall trend of the data, but the points plotted in these instances are probably not representative of their height intervals and have been discounted because of the small number of samples from which they were computed. Table V.III gives the number of samples used in computing the average percentages for each height interval. It can be seen from this that the lowest and three highest height ranges, which contain the erratic points, were sampled only one-third, or less, as often as most of the other intervals. This number of samples was apparently too small and not sufficiently distributed in time to average out the diurnal, seasonal, and magnetic influences, but it should be made clear that the nature of the extraneous influences is not well enough understood to test these points rigorously.

TABLE V.III

| <u>Height Range km</u> | <u>Number of Samples</u> | <u>Height Range km</u> | <u>Number of Samples</u> |
|----------------------------|------------------------------|----------------------------|------------------------------|
| 200-250 | 25 | 750-800 | 76 |
| 250-300 | 78 | 800-850 | 70 |
| 300-350 | 77 | 850-900 | 70 |
| 350-400 | 81 | 900-950 | 61 |
| 400-450 | 85 | 950-1000 | 61 |
| 450-500 | 78 | 1000-1050 | 45 |
| 500-550 | 76 | 1050-1100 | 27 |
| 550-600 | 77 | 1100-1150 | 18 |
| 600-650 | 86 | 1150-1200 | 14 |
| 650-700 | 80 | 1200-1250 | 23 |
| 700-750 | 75 | | |

In an attempt to perform a limited test of the reliability of the data given in Fig. V.6, a scatter diagram of satellite height and closest approach time was plotted. This showed the sampling for the height intervals between 250 and 1050 km to be reasonably well distributed over 24 hours. The occurrence of scintillation as a function of height curves were also plotted separately for summer, winter, and equinoctial months, and, although the scatter of the points increased, the general form of the altitude dependence was preserved. These two tests indicated that the nature of Fig. V.6 was probably not significantly affected by diurnal and seasonal effects except at the extreme low and high altitudes.

4. Discussion

The altitude dependence of scintillation given in Fig. V.6 is interpreted as showing the height distribution of irregularity occurrences, but it should be emphasized that this explanation does not follow from Fig. V.6 alone. For instance, it might be possible to interpret the altitude dependence of scintillation in terms of irregularities occurring in a single thin layer whose effectiveness in producing scintillation increases with increased distance of the satellite above the layer. However, the distribution of heights as measured by the spaced receiver technique (Table V.I) gives support to the former rather than the latter model.

Thus, it is concluded that the bulk of ionospheric irregularities occur below 650 km. They seem to occur with about equal probability between the heights of 250 and 650 km, and their presence at greater heights is sporadic.

The heights given here are considerably greater than have been reported elsewhere, but this may only be a reflection of the fact that in the auroral zone the ionosphere is in general more disturbed than elsewhere and that ionospheric irregularities are both more strongly developed and extend to greater heights.

It might be noted that Bates^{8,9} observed F-layer irregularities at College from 250 to 400 km using the backscatter sounding technique. However, this technique is limited to detection of irregularities below the F2 maximum, so the results are consistent with those reported here.

References

- 1 Briggs, B. H., A Study of the Ionospheric Irregularities which cause Spread-F Echoes and Scintillations of Radio Stars, J. Atm. and Terrest. Phys. 12, 34, 1958.
- 2 Slee, O. B., Radio Scintillations of Satellite 1958 α , Nature, 181, 1610, 1958.
- 3 Kent, G. S., High Frequency Fading Observed on the 40 Mc/s Wave Radiated from Artificial Satellite 1957 α , J. Atm. and Terrest. Phys. 16, 10, 1959.
- 4 Yeh, K. C., and G. W. Swenson, Jr., The Scintillation of Radio Signals from Satellites, J. Geophys. Research, 64, 2281, 1959.
- 5 Parthasarathy, R., R. P. Basler, and R. N. DeWitt, A New Method for Studying the Auroral Ionosphere using Earth Satellites, Proc. IRE, 47, 1660, 1959.
- 6 Little, C. G., Robert P. Merritt, G. C. Rumi, Ernest Stiltner, Rene Cognard, Radio Properties of the Auroral Ionosphere, Geophysical Institute of the University of Alaska, Quarterly Progress Report Nos. 1-5, 7, 8, Contract No. AF 30(635)-2887, Project No. 5535 - Task 45774, 1958.
- 7 Little, C. G. and A. Maxwell, Scintillation of Radio Stars during Auroral and Magnetic Storms, J. Atm. and Terrest. Phys. 2, 356, 1952.
- 8 Bates, Howard F., The Height of F-Layer Irregularities in the Arctic Ionosphere, J. Geophys. Research, 64, 1257, 1959.
- 9 Bates, Howard F., Correction to the Paper, The Height of F-Layer Irregularities in the Arctic Ionosphere, J. Geophys. Research, 65, 1304, 1960.

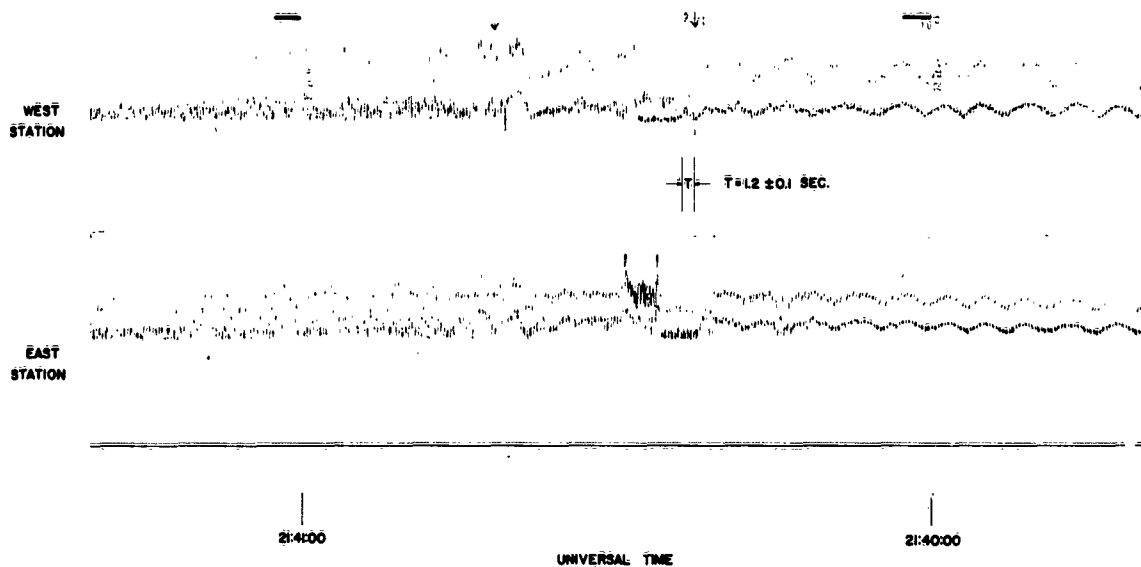


Fig. V.1 Example of spaced receiver recordings from which a height measurement was made. These recordings were made on December 12, 1959, and the height measured in this case was 430-460 km.

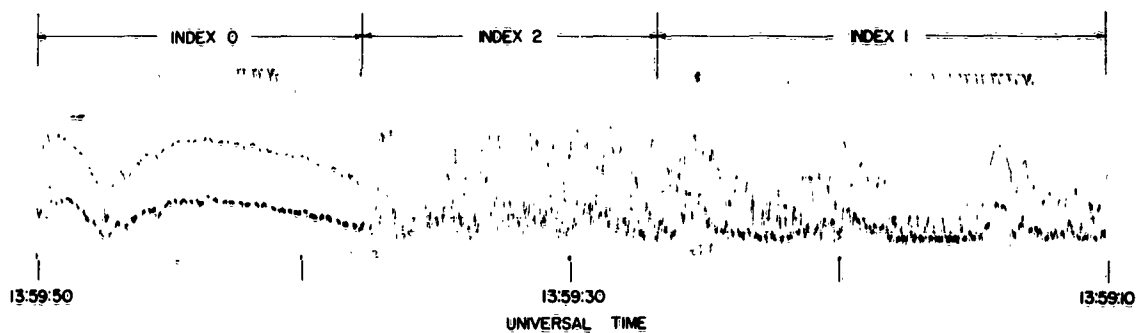


Fig. V.2 Signal strength recording showing examples of all three scintillation indices. The recording was made on June 26, 1958.

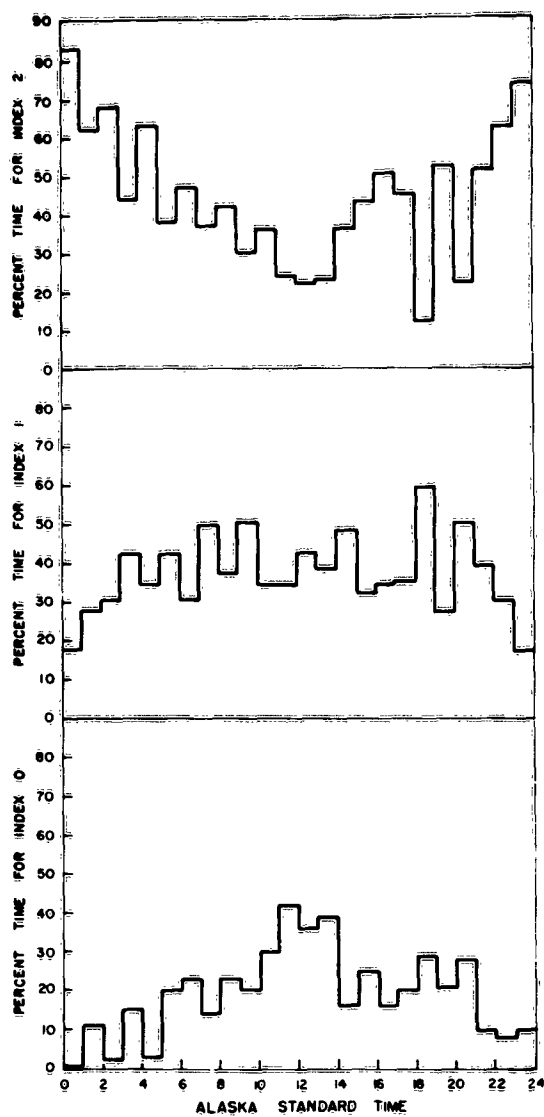


Fig. V.3 Diurnal variation of scintillation indices 0, 1, and 2.

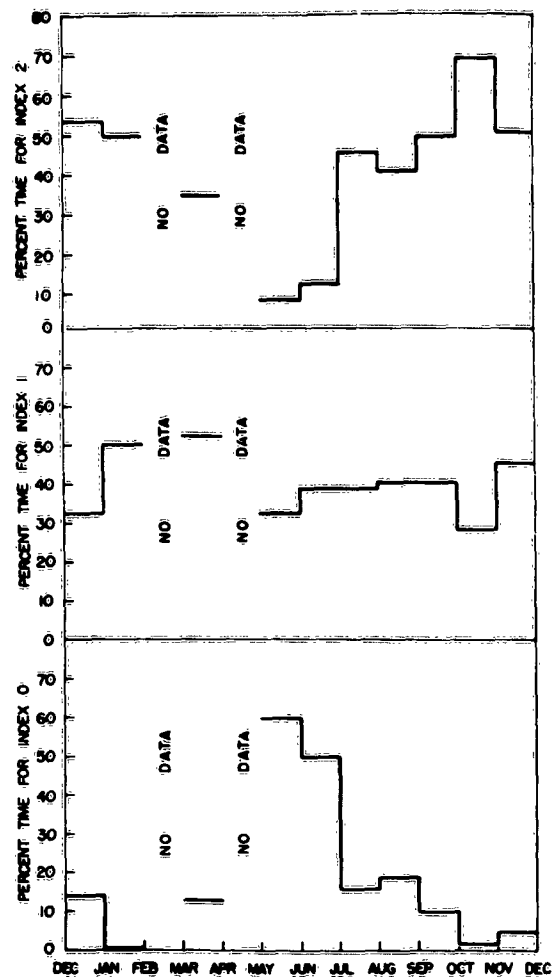


Fig. V.4 Seasonal variation of scintillation indices 0, 1, and 2.

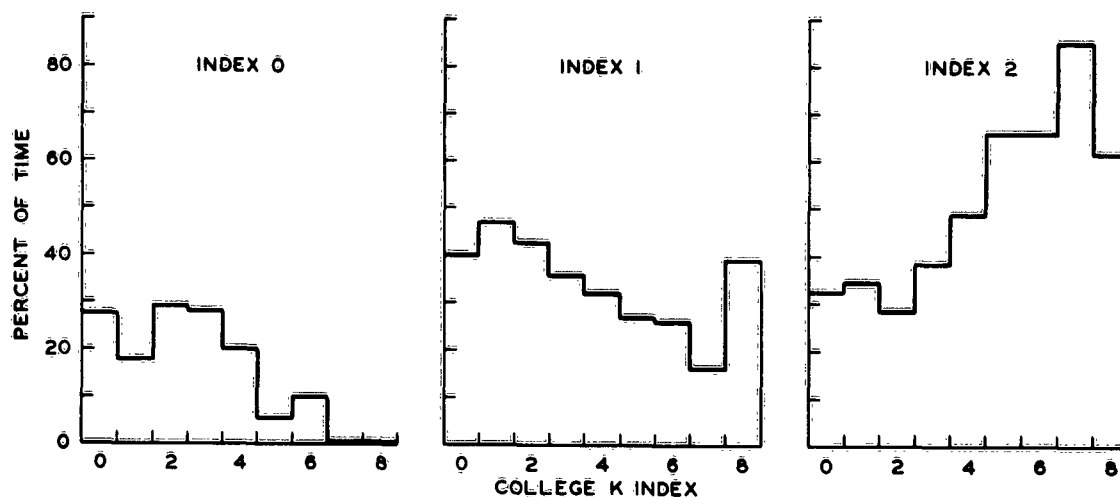


Fig. V.5 Variation of scintillation indices 0, 1, and 2 with College K-Index.

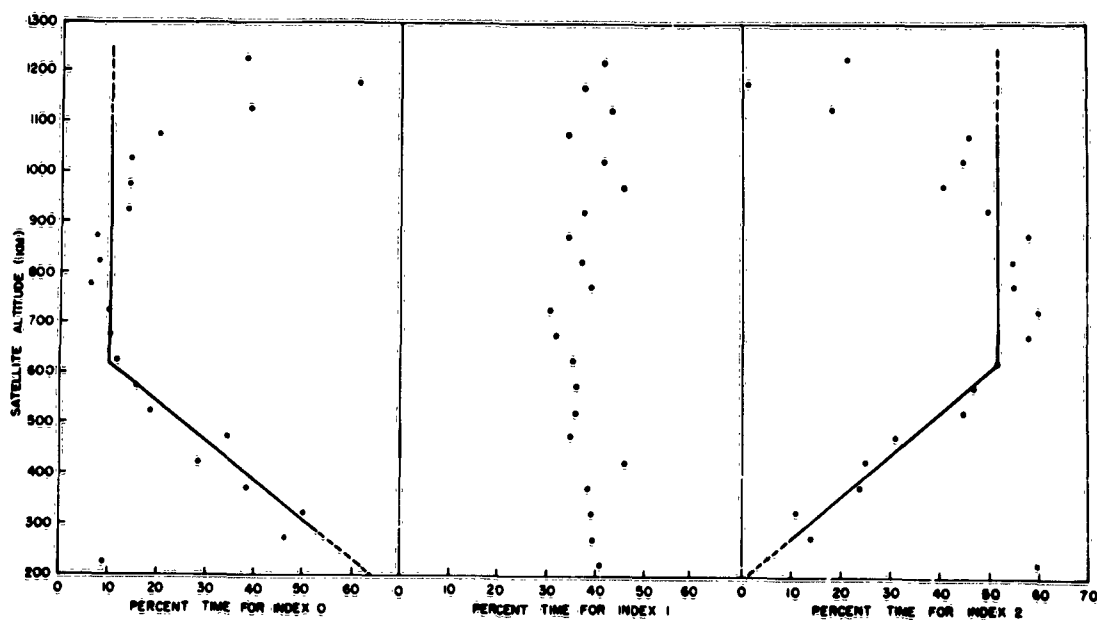


Fig. V.6 Dependence of scintillation indices 0, 1, and 2 on satellite altitude. The straight lines represent the idealized dependence which would be observed if irregularities occurred with equal probability below 650 km and were absent at greater heights.

VI SATELLITE RADIO SIGNAL DETERMINATIONS OF UPPER F REGION ELECTRON DENSITIES IN THE AURORAL ZONE

by

W. B. Murcray and J. H. Pope

The Soviet satellites have been launched in orbits which are particularly well suited for studies of the ionosphere in Alaska. An inclination of about 65° and an argument of perigee of approximately 60° means that the satellite is just coming out of perigee as it passes over central Alaska. The perigee altitudes were around 250 kilometers, and eccentricities around 0.1, which resulted in the satellites rising through a considerable portion of the F region while they were observable from College.

The beacon frequencies of 20 and 40 megacycles are quite well suited to study of this region because they are high enough to penetrate the F region and low enough to be considerably affected by it. In the second satellite (1957B) the keying system quit operating soon after launch, and it transmitted continuous wave signals. These are well adapted to observations requiring frequency measurement because of the absence of switching transients.

A transmitter which is moving with a radial velocity of approach \dot{r} relative to the observing station and transmitting a frequency F into a medium of refractive index n at rest relative to the observing station, will be received at a frequency $F + D$, where D is given by $D \doteq \frac{\dot{r}}{c} nF$, c being the velocity of light in free space¹. Since: $n = (1 - \frac{e^2}{\pi m F^2} N)^{1/2}$ by the Eccles-Larmor equation where e and m are the charge and mass of the electron and N is the electron density in electrons/cm³, it is evident

that if D is measured and \dot{r} and F are known, one can determine N . This procedure is commonly used to measure electron densities from rockets². However, if this method is used, one must know \dot{r} accurately and also F , neither of which can be assumed known with much precision in the case of a satellite.

In the case of a satellite, there is an additional complication because of the large transverse component of velocity involved. The index of refraction is nearly unity except in the ionosphere, and the optical path length at a given distance r will vary depending upon the proportion of the path lying within the ionosphere. This results in changes of optical path length because of the transverse motion of the satellite as well as its radial motion, and hence introduces a spurious addition to \dot{r} . This addition is proportional to time variation of $\int N dr$ between satellite and observing station, and would be an additional source of information provided it could be separated from the other effects.

The Russian satellites transmitted on two frequencies. If we let F_1 be the frequency of the 20 megacycle transmitter and F_2 that of the 40 Mc one, then D_1 and D_2 are the corresponding Doppler frequencies. The ratio of these Doppler frequencies then is

$$\frac{D_1}{D_2} = \frac{F_1}{F_2} \left(\frac{\dot{r}}{c} n_1 \right) \left(\frac{c}{F} n_2 \right) = \frac{n_1}{n_2} \frac{F_1}{F_2}$$

\dot{r} does not appear in this equation, but it should be noted that since \dot{r} is changing with time, it is necessary that the Doppler frequencies D_1 and D_2 be measured simultaneously if the \dot{r} 's are

to cancel. In practice, this requirement is a source of considerable trouble.

Substituting for n_1 and n_2 from the Eccles-Larmor equation and solving for N one obtains:

$$N = \frac{F_2^2 \left\{ \left(\frac{F_1}{F_2} \right)^2 - \left(\frac{D_1}{D_2} \right)^2 \right\}}{1 - \left(\frac{D_1}{D_2} \right)^2} \times \frac{10^{-6}}{80.5} \text{ electrons/cm}^3$$

A little experimentation with this equation shows that N is not very sensitive to errors in F_1 and F_2 , provided that some means exists for accurate determination of the ratio $\frac{D_1}{D_2}$.

Observations of satellite Doppler curves are made by mixing the signal from the satellite with a signal from an oscillator at the observing station. The result is a beat note of frequency Δf , which is the difference between the local oscillator of frequency f and the frequency of the signal received from the satellite. The local oscillator cannot be set exactly on the satellite frequency, so the most convenient technique is to use a local oscillator frequency above the highest frequency expected from the Doppler shifted satellite signal, or below the lowest one. If the local oscillator frequency is less than the lowest frequency from the satellite, then the Doppler frequency becomes:

$$D = f + \Delta f - F$$

and the ratio:

$$\frac{D_1}{D_2} = \frac{f_1 + \Delta f_1 - F_1}{f_2 + \Delta f_2 - F_2}$$

f can be determined within a few cycles/sec, and since D is very small in the vicinity of the time of closest approach when \dot{f} approaches zero, the quantity $f-F$ can be determined to the same accuracy as Δf , even though the time of closest approach is not known exactly and neither satellite nor local oscillator frequencies are known to anything like this precision. Consequently, the ratio $\frac{D_1}{D_2}$ can be determined with considerable accuracy, provided only that both satellite and local oscillator frequencies remain reasonably constant over the period of one satellite passage.

In the observations made by the Geophysical Institute on 1957 β , the beat frequencies on 20 and 40 Mc were recorded on two channels of a three-channel Ampex Tape recorder. A time signal from WWV was recorded on the third channel. The data were reduced by making sonagraph (audio frequency spectrogram) records, which showed the two beat frequencies along with the WWV time signal on the same record. Time resolution was about 0.01 second in absolute time, and measurements of the beat frequencies could be made simultaneous to about the same accuracy. The accuracy of the absolute time was not so important since it was only used to determine the position of the satellite at the time of the measurement, and the orbital data were not sufficiently precise to require 0.01 second accuracy. However, it is extremely important that the beat frequency measurements be matched in time as closely as possible. Satellite positions were obtained from data furnished by the Smithsonian Astrophysical Observatory³.

The spurious Doppler shift introduced by the transverse motion of the satellite through the ionosphere can be roughly calculated¹, and the observed frequency corrected to take account of it. In the passages used in the present calculations this effect is small compared to the effect of local electron densities at the satellite during most of the run. If the local electron densities are small, or if \dot{r} is small, the transverse motion effect becomes comparable to or greater than the local effect, and the electron densities derived by this method become very uncertain. In practice, it has not proven possible to measure electron densities below about $10^5/\text{cm}^3$. The difficulty is a combination of the accuracy with which the corrections can be computed and the accuracy of the beat frequency measurement. It is evident that this imposes fairly severe limitations upon the portion of the orbit over which this method of calculating local electron densities is useful. Where it can be used, it is simple and straightforward, and the calculations easy.

Near the time of closest approach of the satellite, \dot{r} is small, and the results again become uncertain for the same reasons as in the case of low electron density. In this case, however, the situation can be improved. At the time of closest approach the slope \dot{D} of the Doppler curve becomes a maximum.

If \dot{r} is small, one can write for the ratio of the slopes:

$$\frac{\dot{D}_1}{\dot{D}_2} = \frac{n_1 F_1}{n_2 F_2}$$

the subscripts again distinguishing the quantities pertaining to a particular frequency.

This gives the same equation for the local electron density as was derived before except that D_1/D_2 has been replaced by \dot{D}_1/\dot{D}_2 . It is useful in the region in which \dot{r} is small. In the region in which \dot{r} is large the slope is small, so the two methods of measurements are complementary. The slopes are somewhat more difficult to measure than are the beat frequencies. The slopes are also affected by the change in the optical path due to the transverse component of satellite motion, the effect introducing a correction, which is in general of the same order as in the case of the Doppler frequencies, though somewhat more complicated to calculate. This method then, is also limited by low electron densities.

Fig. VI.1 shows an electron density versus height profile obtained by the foregoing methods. Since the satellite was headed nearly due east at this latitude, it traversed approximately ten degrees of longitude per minute. As a result there is a local time difference of about two hours between the sub-satellite points at the lowest and highest altitudes indicated on the figure. This means that what is represented on the figure as a vertical variation only, is a combination of vertical and horizontal variations. This is illustrated in Fig. VI.2 in which the geometry of the passage is sketched.

The day on which the data of Fig. VI.1 were obtained was magnetically quiet, and the ionograms show no disturbance. Consequently, it is probable that conditions at the west end of the path correspond roughly to those at Fairbanks an hour earlier, and at the east end conditions would be like those of Fairbanks

an hour later. Ion densities shown in the lower layer in Fig. VI.2 are obtained from the College C-3 records on this assumption. The true height of the F region maximum at College, as computed from the ionograms was about 290 kilometers. The satellite was well above this on its closest approach to College, which was some thirty miles to the north. It should be noted that Fig. VI.1 shows two distinct layers with a pronounced minimum between, the second layer having a slightly lower electron density than the first, so that it is not visible on the C-3 records. All profiles computed to date are consistent with this structure, although most of the observed runs are at too high altitude to show the lower region which contains the zone of maximum electron density.

Fig. VI.3 shows another profile at a somewhat greater altitude. This run was on a mildly disturbed day. The satellite had passed the most northerly point of its orbit and was heading a little south of due east as it passed College. The profile is definitely consistent with the satellite rising from the low ionization region into the second highly ionized layer. All the points on this profile are high above the F layer maximum.

More satellite passages are being analyzed and it is hoped that a report on the results may be made soon. It is not known whether the two layer structure shown is characteristic for this latitude in winter or whether it is a temporary condition, perhaps present only in the fall. The low electron density in the region between the two maxima is also of interest. In this region the densities were lower than could be measured by the

technique employed, which means that they were not greater than about 10^5 electrons/cm³.

Fig. VI.4 shows densities to a higher altitude than either of the preceeding figures.

Appendix VI.1

Doppler Shifts in Ionized Media

There seems to be a good deal of confusion about the mechanics of the Doppler shift, most of which is probably traceable to the way in which it is generally presented. The treatment normally starts by presenting the equation for the Doppler shift as the result of a relativistic transformation, which gives the received frequency in terms of the transmitted frequency, and the radial velocity of the transmitter relative to the observer¹. The radial velocity is then interpreted as the time rate of change of the phase path, and the treatment carried on from there. This is the natural way to approach the problem, but it has the disadvantage of obscuring the physical mechanisms involved.

Satellite velocities are far from relativistic anyhow, and as we shall see, the simple classical treatment in this case leads to the correct relativistic equations to within terms of the order of $\left(\frac{\dot{r}}{c}\right)^2$. (consideration of the basic axioms of relativity will show that it should) The classical treatment also has the advantage of presenting a clear physical picture.

Suppose the transmitter to be moving through a medium of refractive index n (phase index) with a radial component of velocity of approach \dot{r} relative to the observing station. The transmitter is sending a continuous frequency f . Then in one second the satellite will have advanced a distance \dot{r} toward (or away from, depending upon the sign of \dot{r}) the observer. The wave transmitted at the beginning of the second has advanced a distance $\frac{c}{n}$. There are, therefore, f waves in the distance: $\frac{c}{n} - \dot{r}$ so that the

observed wavelength is $\frac{\frac{c}{\dot{n}} - \dot{r}}{f}$ and the observed frequency:

$$f' = \frac{\frac{c}{\dot{n}}}{\frac{\frac{c}{\dot{n}} - \dot{r}}{f}} = f \frac{\frac{c}{\dot{n}}}{\frac{c}{\dot{n}} - \dot{r}}$$

or: $f' = f \left(\frac{1}{1 - \frac{\dot{r}\dot{n}}{c}} \right)$ multiplying numerator and denominator by

$$\left(1 + \frac{\dot{r}}{c} \dot{n} \right) \text{ one obtains the equation } f' = f \left[\frac{1 + \left(\frac{\dot{r}\dot{n}}{c} \right)}{1 - \left(\frac{\dot{r}\dot{n}}{c} \right)^2} \right]$$

This is the same equation as the one derived by using the Lorentz transformation within a correction which is smaller than $\left(\frac{\dot{r}}{c} \right)^2$. For satellite velocities, $\left(\frac{\dot{r}}{c} \dot{n} \right)^2 \ll 1$ and the Doppler shift is: $f - f' = \frac{\dot{r}\dot{n}}{c}$. This is the so-called "local" Doppler shift, and in many cases is the only one existing. If the medium is homogeneous of refractive index n all the way to the observer, for instance, or if the transmitter moves directly toward or away from the observer, $\dot{r}\dot{n}$ represents the total rate of change of the phase path, and there is nothing more to be said. The satellite will approximate the latter condition when it is far away, and at closest approach \dot{r} becomes zero and there is no Doppler shift, but in the region between these extremes the situation becomes more complicated because the phase path is in part in the ionosphere and part outside so that n varies along the path, and as the satellite moves horizontally the relative amount of path through strata of different n will vary also, so that an additional term must be added to $\dot{r}\dot{n}$ to express the total rate of change of phase path length. At the frequencies employed by

satellites so far, \dot{n} is by far the dominant term, the term involving $\frac{d}{dt} \int n dr$ being a small correction only. However, in deriving electron densities, one uses the fact that n at the satellite differs from the free space value unity, and depending upon conditions the effect of the integral term may become more important than the effect of the difference of the local index at the satellite from unity. Such a case for instance occurs with the satellite above the ionosphere, where the electron density is small.

Treatment of the case of a variable index of refraction is complicated by the fact that the propagation path is not a straight line but the effect in the case considered is not large.

References

- 1 Berning, W., "Scientific Uses of Earth Satellites", edited by Van Allen University of Michigan Press, Ann Arbor, 1956.
- 2 Newell, Homer E., "High Altitude Rocket Research", Academic Press, New York, 1953.
- 3 Adams, R. M., R. E. Briggs and E. K. L. Upton, "Positions of Satellite 1957 β One During the First 100 Revolutions", Smithsonian Institution, Astrophysical Observatory, Special Report No. 16, Optical Satellite Tracking Program, Cambridge, 1958.

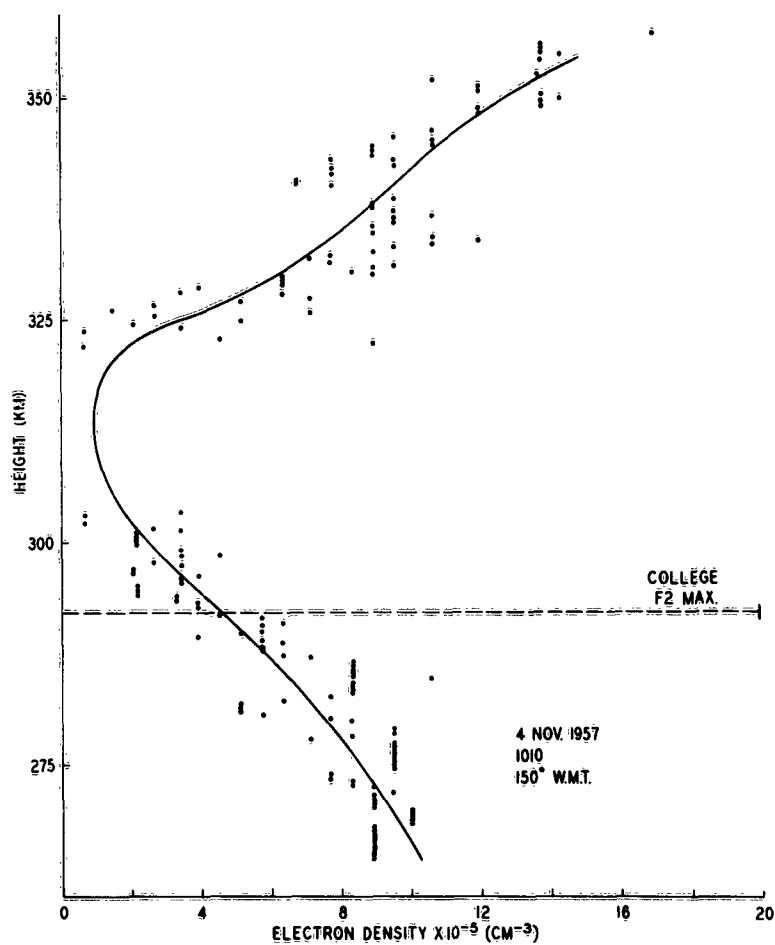


Fig. VI.1 Electron densities over Alaska 4 Nov 1957 (1010 (150° WMT))

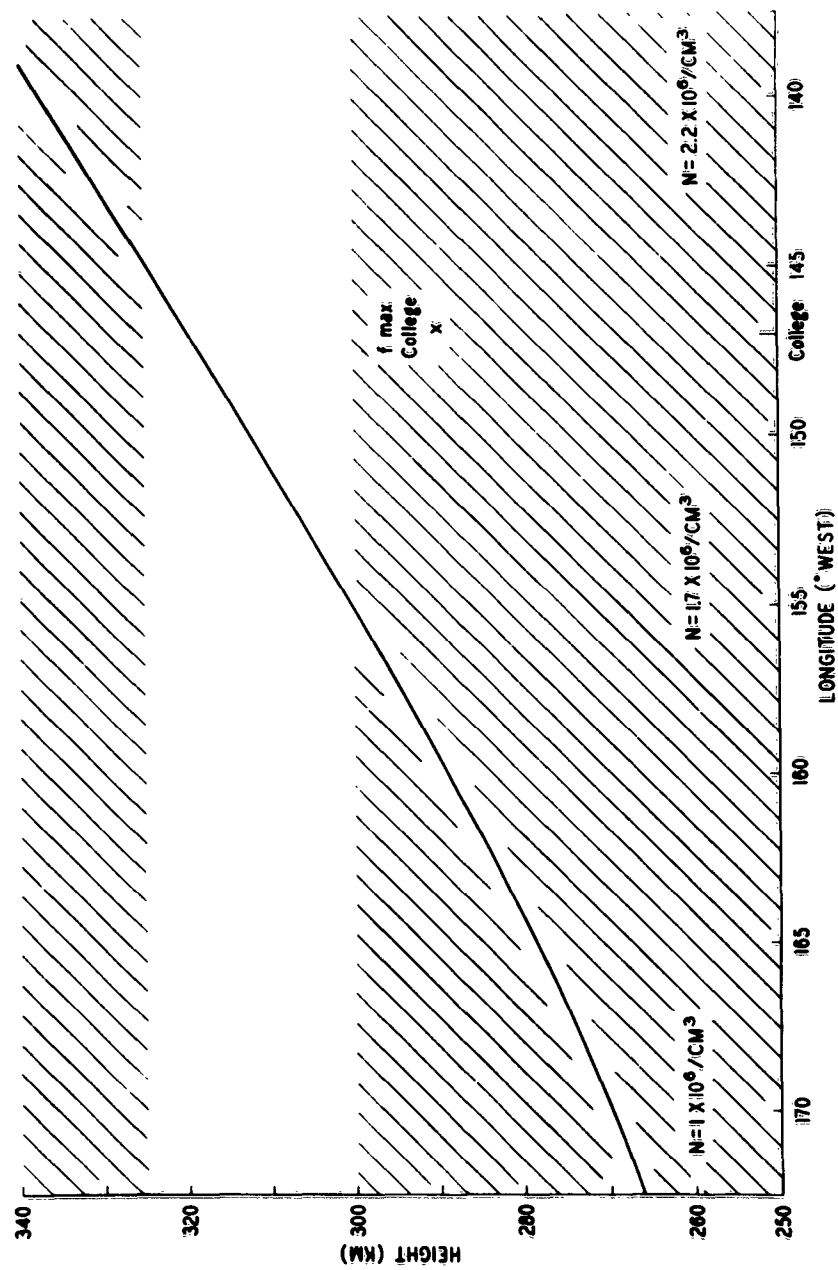


Fig. VI.2 Geometry of satellite pass 4 Nov 1957 1010 (150 WMT)

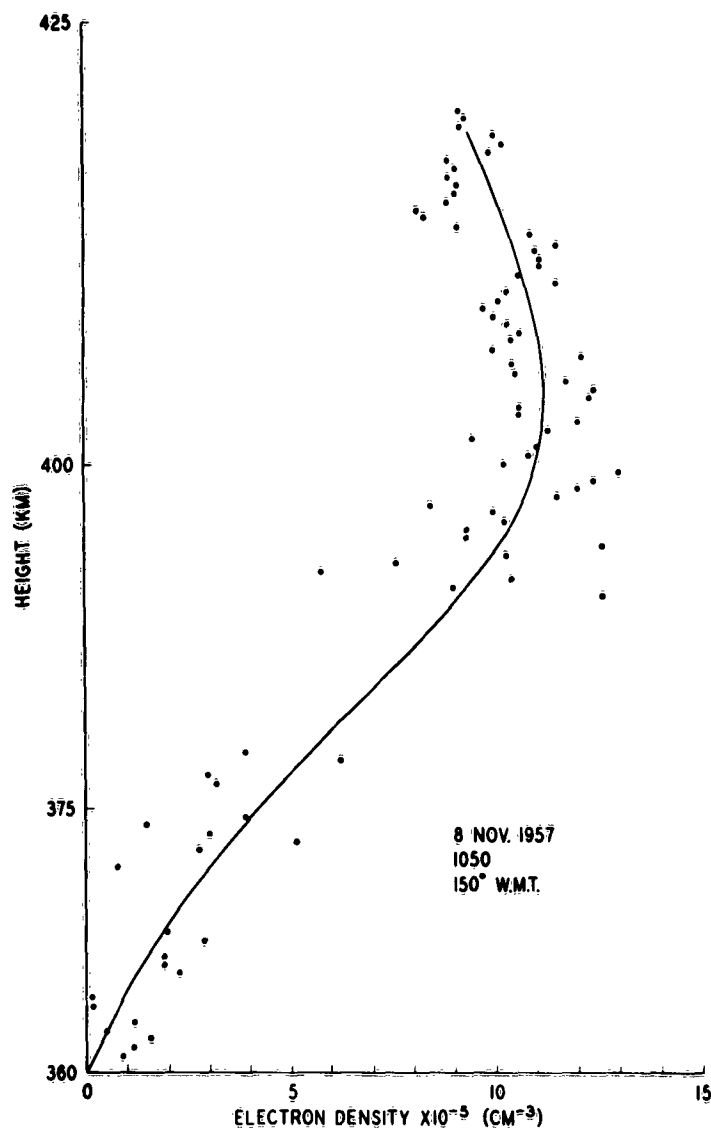


Fig. VI.3 Electron densities over Alaska
8 Nov 1957 (150°WMT)

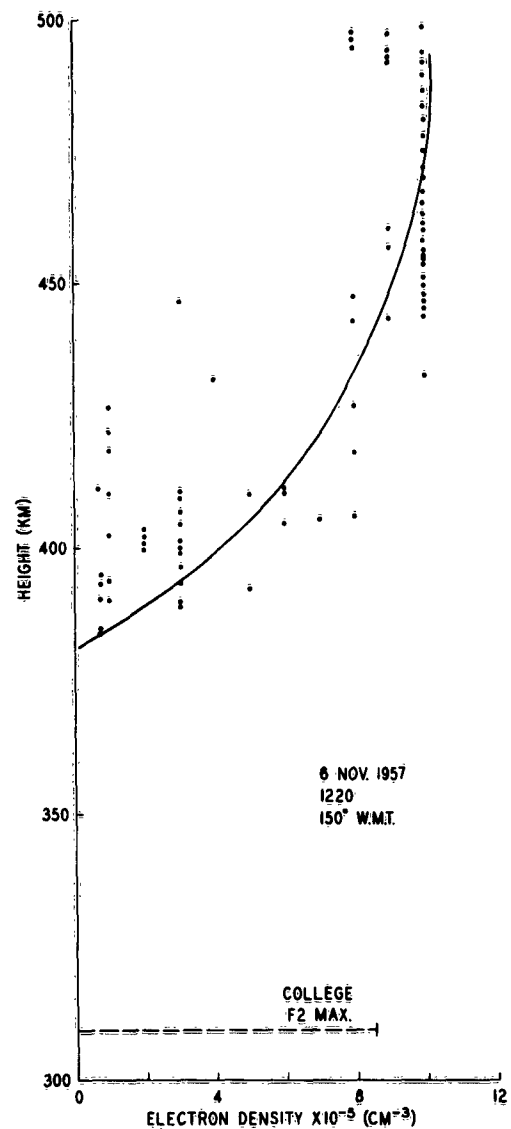


Fig. VI.4 Electron densities
over Alaska 6 Nov 1957 (150°WMT)

VII OBSERVATIONS OF HIGH LATITUDE RADIO AURORA

by

Leif Owren

1. Introduction

The purpose of Section VII is to survey observations of radio aurora made in Alaska, and in particular, the observations from College, Alaska. Some recent results from IGY studies of the visual aurora in Alaska are also reviewed briefly since they have a bearing on the interpretation of the radio observations. Radio aurora has been studied experimentally in this area over nearly a decade, both by visiting and resident scientists. The frequency range covered in course of these investigations extends from high frequencies well into the ultra-high frequency band. Specifically, radio aurora has been studied with pulse techniques in seven different frequency intervals from 12 to 780 Mc/s and by cw techniques on four frequencies from 40 to 400 Mc/s. A representative picture of the high latitude radio aurora can therefore be drawn from the Alaska observations. The regional limitation of our survey has the advantage that the observations referring specifically to the College observations - are uniform in the important geometrical aspects imposed by the earth's magnetic field and the location of the auroral zone. College, Alaska is located in geomagnetic latitude 64.5°N and near the southern border of the auroral zone. It is about 200 km south of the line of maximum occurrence of visual aurora as determined by Vestine¹. The magnetic dip at College is 77° .

2. Visual Aurora in High Latitudes

It is probably well known that a visual auroral display usually starts with the formation of a homogeneous arc. In the auroral zone one generally sees a double arc, consisting of two similar structures parallel to each other. Davis^{2,3} has recently found from IQY studies in Alaska that the two arcs are connected by a loop at their eastern end. The looped arc system is actually stationary in space, with the earth rotating under it (see Fig. VII.1). The western part is quiescent and the eastern part active with the arc broken up into rays and curtains. At a given location south of the center line of the auroral zone, a quiescent period lasting for an hour or more is therefore usually followed by a period when the active section of the arc structure comes into view. During this so-called breakup period a given station may see a complete transformation of the rayed arc into curtains and rays. Following the breakup which usually occurs around magnetic midnight, an eastern branch of the auroral structure consisting mostly of diffuse forms of luminosity rotates into view. Towards morning the discontinuous, diffuse forms may reform into arcs connected at their western end. At a given station south of 66.5° geomagnetic latitude a development of the auroral display involving three phases will be observed. The three phases are characterized by the initial quiescent arcs, the peak of activity during breakup, and the post breakup period of diffuse aurora.

The arcs with their associated forms generally move as a whole in the North-South direction. Actually, for each auroral

display a discontinuity in the direction of the overall motion can usually be found somewhere between the geomagnetic latitudes 62° and 70° . The aurora forming south of this discontinuity shows a (first) motion southwards whereas the aurora forming north of it tends to move northwards; see Davis and Kimball⁷. The detailed structure such as rays and curls appearing in an arc move along it in a clockwise direction. This clockwise motion changes to a counterclockwise direction of motion for the diffuse structures occurring during the post breakup phase, generally after magnetic midnight.

The auroral arcs may be described as thin, wide sheets of luminosity (and ionization) extending a few thousand kilometers parallel to the geomagnetic latitude circles. Vertically an arc extends from about 100 to at least 120 km. The vertical extent is markedly dependent on the sunspot cycle. The width of an arc in the North-South direction is of the order of one kilometer. The rays appearing in an arc, or generally over large areas of the sky during breakup, are always parallel to the direction of the magnetic lines of force, and may extend to great heights, 200 km or more.

3. Radio Aurora in High Latitudes

An early radar observation at Jodrell Bank in 1947, Lovell, Clegg and Ellyett⁴, of auroral echoes on 47 Mc/s were interpreted by Herlofson⁵ in terms of specular reflection from the surface of an (hypothetical) auroral arc. The observed echo range was 480 km, and it has been shown (Chapman⁶) that a radar ray from Jodrell Bank could be normally incident on an auroral arc over the

Faerø Islands at a height of 113 km for the specified slant range. Following this and similar observations, Chapman⁶ worked out the geometry of specular radio reflections from field-aligned auroral forms using an earth-centered dipole to describe the geomagnetic field. Chapman's calculations showed that strictly perpendicular incidence on the undisturbed field configuration at a height of not less than 100 km could not be achieved for high latitude locations above 62° geomagnetic latitude, such as College, Tromsø and Kiruna.

The experimental facts are that transient VHF radar echoes are observed regularly at these high latitude stations during times of visual auroral activity and magnetic disturbances. Generally the echoes are received only in a 90 degree sector centered approximately on geomagnetic north, at low elevation angles, and at fairly long ranges which are typically between 500 and 1000 km. Interferometer and pencil-beam radar determinations of the elevation angles has shown that the heights of the echoing centers tend to cluster in the interval from 100 to 110 km regardless of the geomagnetic latitude of the observing station. As these experimental results accumulated they raised interpretational problems which were discussed extensively during the last decade and which are perhaps not even today finally resolved. We do not wish to dwell on theories which were found to be untenable before 1957, but shall concentrate on ideas which have been under consideration during the last three years and may provide a proper basis for further discussions.

The experimental findings clearly make it necessary to modify in some way the original theory of specular reflection from auroral forms aligned with the undistorted geomagnetic field. One line of thought is to maintain the condition of strictly perpendicular incidence of the radio waves on field-aligned auroral structures and to achieve this perpendicularity either by distortion of the magnetic field or by ray-bending in the E layer. A second approach, and thus far the most successful, is to weaken the condition of strict perpendicularity and replace the specular reflection by backscatter at nearly perpendicular incidence. This theory was suggested by Moore^{8,9}, extended by Booker, Gartlein and Nichols¹⁰, and subsequently developed mathematically by Booker¹¹. The theory of scattering from field-aligned electron density irregularities introduces the notion of "aspect sensitivity" in auroral scatter of radio waves. In this theory the largest "off-perpendicular angle" at which a radio wave can be incident on the field direction and yet produce a detectable scatter signal becomes an important parameter. A third idea, advanced by Forsyth^{12,13} is a hybrid type theory whereby the radar echoes may be returned partly by pure volume scattering in auroral ionization without recourse to field-aligned irregularities, and partly by specular reflections or scatter from field-aligned auroral luminosity.

Consideration of the available experimental evidence (see Appendix) indicates that neither the distortion of the magnetic field nor the average electron density of the auroral E layer is sufficient to re-establish the theory of specular reflection

from field-aligned auroral forms. The accumulated body of knowledge concerning both visual and radio aurora tends to contradict the theory of pure volume scattering from auroral ionization. For future reference we quote (see Appendix) the following results for the electron density in the auroral E layer. HF soundings at vertical and oblique incidence indicate that the average electron density of that part of the E layer which can be so explored corresponds to a plasma frequency of about 4 Mc/s or 2×10^5 electrons/cm³. Photoelectric measurements of the luminous aurora indicate that for moderately bright forms there exists in limited volumes an electron density of about 10^6 electrons/cm³, corresponding to a plasma frequency of about 10 Mc/s. For very bright forms the electron density may be as high as 10^7 electrons/cm³, corresponding to a local plasma frequency of about 30 Mc/s.

4. Theory of Scattering in Field-Aligned Irregularities

The scattering theory developed by Booker¹¹ is a statistical volume scattering theory where the individual scattering elements are non-isotropic electron density irregularities. The irregularities are represented as elongated, axially symmetric bodies of plasma. The probability of finding at a given point in the plasma a deviation, ΔN , from the average local value, N , is assumed to be given by an error law. More precisely, the autocovariance of the relative deviation in capacitivity, $\Delta\epsilon/\epsilon$, is assumed to be a gaussian function. The theory further assumes that the incident radiation field is only weakly perturbed by the electron density irregularities. Certain implicit assumptions

of the theory should be explicitly stated.

1. The refractive index of the medium seen by the incident radio waves must be approximately equal to unity, $\mu \approx 1$.
2. The relative deviation of the electron density in the medium, $\Delta N/N$, as well as the local average electron density, N , itself must be spatially stationary stochastic variables, i.e. statistically uniform quantities, over the scattering volume.

The assumption about the refractive index implies that the theory is applicable only for frequencies exceeding about 30 Mc/s when the scattering volume is associated with moderately bright auroral forms. It also implies that for very bright forms the observing frequency should not be less than approximately 90 Mc/s. On the whole this assumption leads one to expect that the theory should work well for frequencies above 60 Mc/s and show signs of failing below 60 Mc/s.

The assumption about the statistical uniformity of $\Delta N/N$ and N implies that the theory can only be expected to work reasonably well when small scattering volumes are involved. This further implies that the theory can only be used with confidence on observations made with pencil-beam radars.

Booker used an auto-covariance function of the form

$$(1) \quad \rho(x,y,z) = \exp \left[- \frac{1}{2} \left(\frac{x^2 + y^2}{T^2} + \frac{z^2}{L^2} \right) \right]$$

The theory then leads to an expression for the ratio of the received power, P_R , to the transmitted power, P_T :

$$(2) \quad P_R/P_T \propto \frac{T^2}{\lambda} e^{-8\pi^2 T^2/\lambda^2} \left[1 - \operatorname{erf}\left(2^{1/2} \frac{2\pi L}{\lambda} \alpha_0\right) \right] \frac{1}{\lambda^4} \left(\frac{\Delta N}{N}\right)^2$$

where T is the correlation distance transverse to the axis of symmetry of the irregularities,

L the longitudinal correlation distance (along the earth's magnetic field),

α_0 the "off-perpendicular angle" (complement to the angle between the direction of incidence and the axis of symmetry) at the bottom of the scattering volume,

λ_N the plasma wavelength corresponding to the electron density,

λ the local wavelength of the incident radio wave in the medium (assumed equal to the free space wavelength).

The factors relating to the antenna, echo range and area of the scattering volume have been omitted in Equation (2).

The aspect sensitivity is characterized by the factor

$$(3) \quad 1 - \operatorname{erf}\left(2^{1/2} \frac{2\pi L}{\lambda} \alpha_0\right)$$

which depends on the correlation distance along the earth's magnetic field, the off-perpendicular angle and the wavelength. The aspect sensitivity factor determines both the range cut-off and the azimuth cut-off of the auroral echoes. The shortest range should in the northern hemisphere be observed with the antenna beam pointed towards geomagnetic north. By selection of the appropriate value of L the observed variation in range and azimuth cut-off as a function of wavelength should be reproduced if the theory is correct. Conversely, if the theory is assumed to be correct, observational determination of the off-perpendicular angle, α_0 , leads to a value for longitudinal correlation

distance, L . It should be noted that a determination of the off-perpendicular angle, α_0 , must necessarily be based on a model for the earth's magnetic field at E layer heights. Such models may be based on either the simple centered dipole field or the earth's main field. In the latter case one uses the surface field and assumes that the surface values of the magnetic declination and inclination may be used at ionospheric heights. The observations of radio aurora at College, Alaska show that for this location the surface field model provides a better approximation to the actual field than the dipole field model, although the actual E layer field would probably be described best by a hybrid model.

Booker emphasized the point that a single value of the longitudinal correlation distance, L , should suffice to describe the radio aurora observations at all frequencies. This appears to be a point more of mathematical convenience than physical reality. When Booker wrote his paper the goal was to produce a theory which would roughly describe the available observations which then spanned a frequency range of no more than 4:1. For such a program a single value of L was adequate. Today we are concerned with observations which span a frequency range of 15:1 even when we limit ourselves to the frequencies from 60 Mc/s and upwards. It seems physically unreasonable that the electron density irregularities seen by 5 meter waves should have exactly the same longitudinal correlation length as those seen by 30 centimeter waves. Physically it appears more reasonable to admit the possibility of at least some change with frequency of the electron density contours of the scattering irregularities.

The upper frequency limit for detection of auroral echoes is determined by the exponential factor

$$(4) \quad \exp (-8\pi^2 T^2 / \lambda^2)$$

This factor becomes very small when $\lambda \approx 2\pi T$. The intensity variation of the backscattered echoes as a function of frequency therefore permits an observational estimate of the transverse correlation distance T .

We have noted that the refractive index seen by the exploring radio waves in the auroral ionization may start to deviate markedly from unity if we go below about 60 Mc/s. In addition D layer absorption will also increasingly influence the observations as we decrease the frequency below 100 Mc/s, and this influence should become very noticeable from 60 Mc/s and downwards. The absorption will affect the observed range and azimuth cut-offs, in particular the latter which will be underestimated. As a consequence the largest observable off-perpendicular angle will be underestimated, and the longitudinal correlation distance should appear to increase systematically with increasing wavelength. One may therefore predict that an experimentally determined curve for the frequency variation of the longitudinal correlation distance should show a turning point at about 60 Mc/s.

5. High Latitude Observations of Radio Aurora

Notable advances have been made in the experimental studies of radio aurora during the last three years. The most outstanding work is probably that carried out by a team from the Stanford

Research Institute at College, Alaska with a pencil-beam radar in the high VHF and the UHF band. A steerable parabolic reflector antenna with a diameter of 61 feet (20 meters) operated with medium power pulse transmitters at the frequencies 216, 398 and 780 Mc/s provided beamwidth of 6, 3 and 1.5 degrees respectively. The most interesting result of the observations is perhaps the discovery of the two types of radio auroral forms, called respectively discrete and diffuse according to the echo appearance, Leadabrand et al¹⁴, Presnel et al¹⁵. The discrete echoes have short duration and are oriented almost vertically in the E layer, typically between 90 and 130 km. These echoes occur mostly at night, when the E layer is in darkness. They often appear to be associated with auroral arcs located some 600 km in the direction of geomagnetic north from College. The diffuse echoes have long duration and are oriented almost horizontally in the E layer, extending over a few hundred kilometers in the magnetic North-South direction. These echoes are almost invariably associated with scattering centers in the sunlit E layer occurring typically in the height interval 90-110 km.

The most frequently occurring height for the scattering centers was found to be 100-110 km in agreement with earlier determinations.

The observed characteristics of both the discrete and diffuse echoes are in complete agreement with those expected from the theory of aspect sensitive scattering.

An interesting question arising in connection with radio aurora is whether aspect sensitive scattering is maintained in

the HF range or simple volume scattering finally takes over. With a steadily weakening aspect sensitivity for decreasing frequency, one should eventually be able to obtain auroral echoes from the south. A high resolution 12.3 Mc/s backscatter sounder with rotating antenna and PPI display was operated at College during most of the year 1957. A study of the records reveals that occasionally during periods of auroral activity a short range E layer echo is returned from all azimuths, Owren and Hunsucker¹⁶. The PPI display shows the echo as forming a complete ring around the station with a typical minimum range in the direction of geomagnetic north of 150 km and a typical minimum range in the direction of geomagnetic south of 250 km. Intermediate range values are obtained in the east and west directions. Thus the echo shows aspect sensitivity and it could be returned either by specular reflection from field-aligned columns after refraction in the auroral E layer or by off-perpendicular backscatter. Refraction calculations show that for the short slant ranges mentioned, specular reflection is not possible and the echo is returned by backscatter at angles between 20 and 30 degrees.

6. Summary and Discussion of College Observations Between 12-800 Mc/s

The main observational facts concerning the College observations over the frequency range from 12 to 800 Mc/s will now be summarized by means of a set of diagrams.

6.1 Diurnal variation

Fig. VII.2 shows the diurnal distribution of auroral echoes

for the three frequencies 12.3, 41 and 216 Mc/s. The 12 Mc/s data are for long range echoes propagated by the F layer in the daytime and the Es layer at night. The coinciding afternoon peaks for the diffuse 216 Mc/s and the 12 Mc/s echoes may be noted.

6.2 Range distribution

Fig. VII.3 is remarkable because it indicates that the range cut-off occurs at the same range of 300 km for all frequencies from 41 up to 398 Mc/s. This result is contrary to the prediction of the theory for aspect sensitive backscatter and requires explanation. Inspection of Fig. VII.4 may help to provide the clue. The solid, slanting line on this diagram indicates the variation in off-perpendicular angle as a function of frequency which results from the SRI studies. The solid horizontal lines represent the range of values tabulated by Peterson, private communication. The 106 Mc/s observation was made at Stanford, California. The broken vertical line results if it is assumed that the echoes having the shortest range are returned from the direction of the geomagnetic north and from a height of 100 km. This is precisely the kind of assumption one has to make in order to deduce the largest off-perpendicular angle from the range cut-off observed with a wide beam radar. The constant value of 7.5° for all frequencies between 40 and 400 Mc/s is then obtained from a contour plot for College of the off-perpendicular intersection angles at a height of 100 km, see Leadabrand et al¹⁴.

The lack of variation in the cut-off range with frequency can be explained by combination of several factors such as

(i) errors in the range measurements, (ii) confusion of the statistics by occasional echoes from height much lower than 100 km (the luminous aurora can at times penetrate as far down as 65 km), (iii) changes in the longitudinal correlation distance with frequency. We must conclude that the observed cut-off range is not a reliable indicator of the aspect sensitivity.

6.3 Azimuth distribution

Fig. VII.5 depicts the observed azimuth distribution and the variation in the azimuth cut-off as a function of frequency. The plot is centered on geomagnetic north, but it will be seen that the histograms tend to peak ten degrees further east which corresponds to the bearing of the magnetic dip pole. The typical 700-800 km range of the echoes having the largest azimuth excursions are indicated. This diagram contains by far the most interesting set of observational data because a well defined law for the azimuth cut-off as function of frequency is indicated. The slanting broken curve provides the means for a determination of the longitudinal correlation distance over a wide frequency range.

6.4 Longitudinal correlation distance

Fig. VII.6 shows the curve for the longitudinal correlation distance, L , as a function of frequency which results from the azimuth cut-off observations. The upper, left hand part of the curve indicates that the longitudinal correlation distance decreases slowly with wavelength between 100 and 800 Mc/s. The predicted turnover at about 60 Mc/s is confirmed, and between 52 and 30 Mc/s a rapid variation of L with frequency is apparent.

This rapid variation does probably not reflect a real variation in L of this magnitude in the scattering medium. What we see must be an indication of the effect of increasing non-deviative absorption as the observing frequency is decreased. The values for the longitudinal correlation distance estimated by Booker¹¹ for the frequency range from 25 to 100 Mc/s in 1956 and determined by Presnell et al¹⁵ in 1959 for the 200-800 Mc/s range is inserted for comparison.

7. Auroral Fading Rates

The literature contains many references to the high fading rates of auroral echoes or aurorally propagated cw signals, but there is a dearth of precise determinations. The curves shown in Fig. VII.7 summarize the available information concerning the frequency variation of auroral fading rates. The solid line represents the "rule of thumb" statement that the fading rate is ten times the frequency in megacycles. The curve was passed through a point resulting from a determination by the Lincoln Laboratories, M.I.T. at about 400 Mc/s, Peterson, private communication. The solid line between 50 and 150 Mc/s is based on observations by Bowles¹⁷. The number of samples are indicated. The broken curve is the result of a recent set of observations from College, Hunsucker, private communication. The observations were made simultaneously on 12 and 18 Mc/s using equipowered transmitters with scaled antennas which illuminated the same scattering volume.

8. Auroral Doppler Shifts

Measurements of the Doppler Shift of auroral echoes have been made at College by Nichols¹⁸ in the VHF range and by Leadabrand

et al¹⁹ in the VHF range. Nichols used two fixed antennas with 3 db beamwidths of 60 degrees oriented at approximately 30 degrees east and west of geomagnetic north and operated at frequencies of 41.15 and 106.0 Mc/s.. He found the major component of the auroral drift to lie in the east-west direction with the predominant motion being westward in the evening and eastward in the morning hours.

Leadabrand et al¹⁹ utilized a steerable antenna having a beamwidth of 3° and operating at 398 Mc/s. They also found that the Doppler shift of auroral echoes was consistent with east-west motion, but in contrast to Nichol's result they found no reversal in the direction of motion near magnetic midnight. A possible explanation of this apparent discrepancy is illustrated in Fig. VII.8. In this diagram are shown the regions from which the Doppler shifted echoes were received by Nichols (lightly shaded area) and by Leadabrand et al (solid black area) relative to the pattern of visual aurora alignment and motion deduced by Davis³. Nichol's antennas received echoes to the northeast and northwest of College because of their fixed orientation. Leadabrand et al observed echoes at somewhat greater range and primarily from the north due to the requirement of near-perpendicularity to the field lines at the higher operating frequency.

It is seen in Fig. VII.8 that the echoes received by Leadabrand et al come from the portion of the visual auroral pattern of primarily southward motion of irregularities along the auroral forms. No abrupt reversal of motion occurs in this portion of the pattern as is the case at positions closer to College.

Near College a reversal in motion from westward to eastward is expected to occur near local magnetic midnight. Using the hypothesis that the direction of motion of the reflecting ionization is that indicated by the motion of the visual aurora, it is reasonable that the difference in the results obtained by Nichols and Leadabrand et al can be attributed to the different regions from which those investigators obtained the Doppler shifted auroral echoes.

9. The Radio Auroral Zone

In conclusion it may be of interest to consider the general distribution of radio aurora over Alaska. A chain of five 41 Mc/s radars was operated in Alaska as part of the IGY auroral program in the U.S. This chain was laid out approximately along a magnetic North-South line between the geomagnetic latitudes 51 and 68.5 degrees such that the visual auroral zone was spanned by overlapping, fixed radar beams. From the distribution of echoing activity as a function of geomagnetic latitude, Leonard²⁰ has deduced a very striking radio auroral zone which is in good agreement with the auroral zone determined from visual observations during IGY. (See Fig. VII.9)

APPENDIX

Distortion of the Magnetic Field

The magnetic observations at College at times of major auroral activity, Heppner²¹, show that at ground level the variations in inclination are no larger than 1-2 degrees even during the most disturbed phase, viz., the negative bay period which coincides with the auroral breakup. Similarly, Størmer's observations in Southern Norway, see Harang²², of the fluctuations in the radiant of corona formations on occasions of very large auroral displays shows that at, say, the 200 km level the inclination changes do not exceed 1-2 degrees. Neither of these observations are necessarily representative of the magnitude of the field distortions at E layer heights. But they indicate that the variations in the dip angle at 100-110 km may fall far short of the fluctuations of the order of 7-15 degrees required to explain the radio observations in terms of a "glint" return of the radio waves at normal incidence. Leonard (private communication) has compared the diurnal variation in inclination at Point Barrow, 800 km northwest of College, with the diurnal variation in occurrence of 41 Mc/s auroral radar echoes observed at College. He finds that the data indicate no close relationship. Although due to lack of E layer magnetic data we cannot reach a final conclusion on the role which magnetic field distortion plays in radio wave returns from auroral ionization, the available evidence indicates that it is not a major factor.

Refraction and Auroral E Layer Electron Densities

Independent studies of the auroral E layer over and near College based on regular vertical incidence soundings by Owren and Hunsucker¹⁶, and oblique, sweep-frequency backscatter soundings, Bates, private communication, both lead to the result that the critical frequencies for the thick layer formations fall inside the range of 2-6 Mc/s, with 4 Mc/s being a representative value. Thus the average electron density of the part of the E layer explored by the 1-25 Mc/s sounders is of the order of 2×10^5 electrons/cm³. This finding does not exclude the possibility that higher electron densities can exist in limited volumes and higher strata of the auroral E layer. But it indicates that ray-bending of VHF waves, which must depend on the average electron density in larger volumes of the E layer, must be slight. The radiation from a 40 Mc/s radar used for studies of radio aurora will under typical conditions be refracted through an angle of less than 2 degrees on traversing a parabolic E layer up to the level of the maximum electron density. Clearly refraction in the auroral E layer cannot bend VHF waves to normal incidence on the field lines in high latitudes.

The electron density in the region of space at the 100 km level which is filled with auroral luminosity can now be fairly accurately estimated from absolutely calibrated photoelectric measurements. Murcray, private communication, finds from College, observations of the auroral emission at 3914A that the electron density is of the order of 10^6 electrons/cm³ for moderately

bright aurora. This corresponds to a plasma frequency of about 10 Mc/s. For very bright auroral forms the electron density is about 10^7 electrons/cm³, corresponding to a plasma frequency of about 30 Mc/s. It was also found by Murcray²³, that the luminosity of the zenithal aurora correlated well with the upper frequency limit (fEs) for scatter observed simultaneously from the auroral E layer with the College vertical incidence sounder.

An interesting HF echo from radio aurora has recently been studied by Bates (private communication) with the oblique incidence 1-25 Mc/s sounder. During disturbed conditions a "slant Es" echo is observed which extends nearly or entirely up to the upper frequency limit. The linear range versus frequency increase levels off at a constant slant range of 500 or 600 km above 20-22 Mc/s. It is found that whenever this backscatter echo extends above 22-23 Mc/s in frequency, an auroral echo is also observed at the same range of 500 or 600 km on the 41 Mc/s radar.

Volume Scattering

It has recently been suggested by Forsyth¹³ that pure volume scattering from auroral arcs which does not in any way depend on field-aligned structure may contribute substantially to the received radar echoes. If this theory were correct one should expect that:

- (a) Echoes were observed from auroral arcs at small zenith distance (large elevation angle) during the first of the three phases of the auroral display. It is known that auroral D layer absorption is low or absent during this phase. The

strong auroral absorption is typically associated with the breakup and the post breakup periods.

- (b) A radar located in higher geomagnetic latitude than the auroral zone, for instance at Point Barrow, Resolute Bay or Thule, should mainly observe auroral echoes from the south. This is due to two circumstances, namely favorable geometry for scatter from an auroral arc in the south which presents a convexly curved target providing a certain focusing effect, and the fact that mostly rayed auroral forms occur north of the auroral zone.

Both these possibilities have been tested in carefully planned and executed experiments by Dyce²⁴ at Point Barrow on 52 Mc/s using both pulse and cw techniques. The results indicated rather conclusively that only aspect sensitive type backscatter occurs.

References

- 1 Vestine, E. H., The Geographic Incidence of Aurora and Magnetic Disturbances, Northern Hemisphere, Terr. Mag., 49, 77-102, 1944.
- 2 Davis, T. N., The Morphology of the Polar Aurora, J. Geophysical Research, 65, 3497-3500, 1960.
- 3 Davis, T. N., An Investigation of the Morphology of the Auroral Displays of 1957-58, Sci. Rept. No. 1, NSF Grant No. G14782, Geophys. Inst. UAG-R117, College, Alaska, 107 pp., 1961.
- 4 Lovell, A.C.B., J. A. Clegg and C. D. Eliyett, Radio Echoes from the Aurora Borealis, Nature, 160, 372, 1947.
- 5 Herlofson, N., Interpretation of Radio Echoes from Polar Auroras, Nature, 160, 867, 1947.
- 6 Chapman, S., The Geometry of Radio Echoes from the Aurorae, J. Atmos. and Terrestrial Physics, 3, No. 1, 1-29, 1952.
- 7 Davis, T. N., and D. S. Kimball, Incidence of Auroras and their North-South Motions in the Northern Auroral Zone, Sci. Rept. No. 4, NSF Grant No. Y/22.6/327, Geophys. Inst., UAG-R100, College, Alaska, 18 pp., 1960.
- 8 Moore, R. K., A VHF Propagation Phenomenon Associated with Aurora, J. Geophysical Research, 56, 85-96, 1951.
- 9 Moore, R. K., IRE Transactions on Antennas and Propagation, No. 3, 217, 1952.
- 10 Booker, H. G., C. W. Gartlein and B. Nichols, Interpretations of Radio Reflections from the Aurora, J. Geophysical Research 60, 1-22, March 1955.
- 11 Booker, H. G., A Theory of Scattering by Non-Isotropic Irregularities with Application to Radar Reflections from the Aurora, J. of Atmos. and Terrestrial Physics, 8, Nos. 4/5, 204-222, 1956.
- 12 Forsyth, P. S., Radio Measurements and Auroral Electron Densities, J. Geophysical Research, 58, 53-66, 1953.
- 13 Forsyth, P. A., On the Geometry of Radio Reflections from Aurora, Canadian J. of Physics, 38, 593-603, 1960.
- 14 Leadabrand, R. L., et al, Preliminary Results of 400 Mc Radar Investigations of Auroral Echoes at College, Alaska, IRE Transactions on Antennas and Propagation, AP-7, 127-136, 1959.

- 15 Presnell, R. I., et al, VHF and UHF Radar Observations of the Aurora at College, Alaska, J. Geophysical Research, 64, 1179-1190, 1959.
- 16 Owren, L. and R. D. Hunsucker, Observations of HF Radio Aurora, Paper Presented at Spring URSI Meeting, 2-5 May, 1960 at Washington, D.C.
- 17 Bowles, K., The Fading Rate of Ionospheric Reflections from the Aurora Borealis at 50 Mc/s, J. Geophysical Research, 57, No. 2, 191-197, 1952.
- 18 Nichols, B., Auroral Ionization and Magnetic Disturbances, Proc. IRE, 47, (2), 245-254, 1959.
- 19 Leadabrand, R. L., R. I. Presnell, M. R. Berg, and R. B. Dyce, Doppler Investigations of the Radar Aurora at 400 Mc, J. Geophys. Research, 64, 1197-1203, 1959.
- 20 Leonard, R. S., Distribution of Auroral Radar Disturbances in Alaska during the IGY, Paper Presented at the URSI Spring Meeting 2-5 May, 1960, at Washington, D. C.
- 21 Heppner, J. P., Time Sequences and Spatial Relations in Auroral Activity during Magnetic Bays at College, Alaska, J. Geophysical Research, 59, No. 3, 329-338, 1954.
- 22 Harange, L., The Aurorae, John Wiley and Sons, Inc., New York, 1951.
- 23 Murcray, W. B., Some Properties of the Luminous Aurora as Measured by a Photoelectric Photometer, J. Geophysical Research, 64, 955-960, 1959.
- 24 Dyce, R. B., Auroral Echoes Observed North of the Auroral Zone on 51.9 Mc/s, J. Geophysical Research, 60, 317-323, 1955.

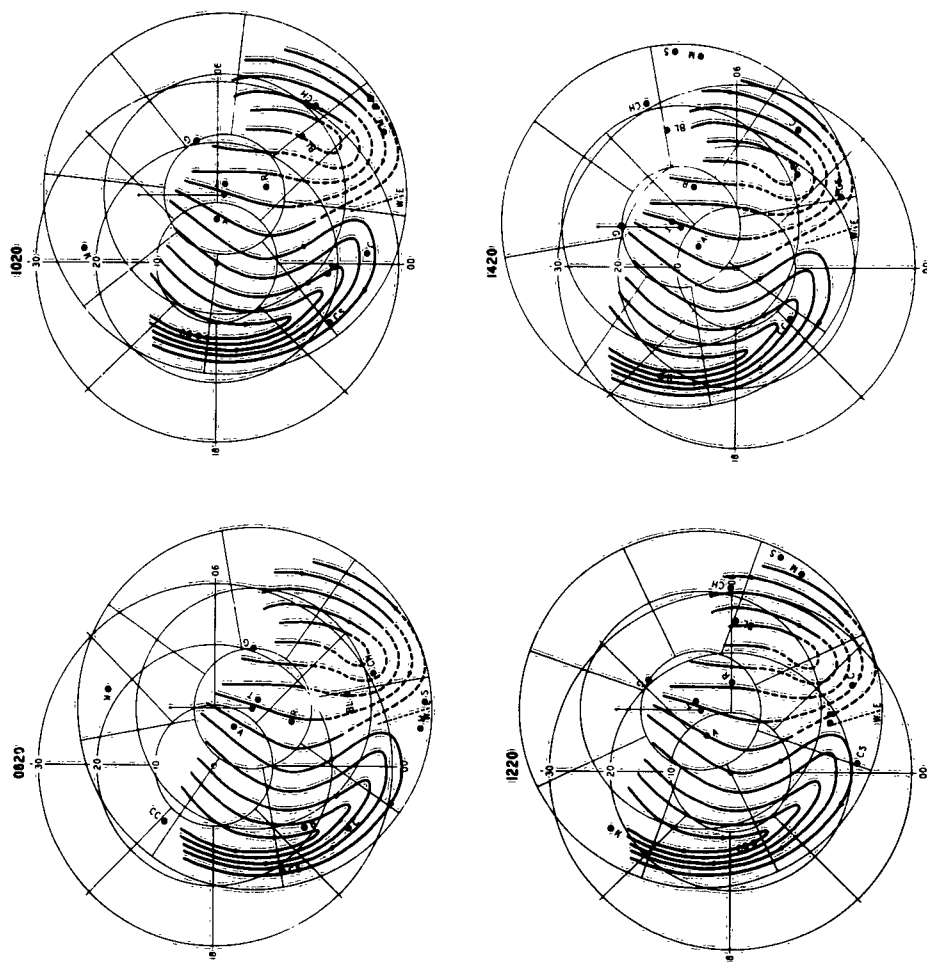


Fig. VII.1 The pattern of auroral alignment and motion deduced for the northern hemisphere and showing the position of 13 high-latitude stations relative to the pattern at 4 universal times. The stations are College (C), Alert (A), Thule (T), Resolute Bay (R), Godhavn (G), Baker Lake (BL), Churchill (CH), Meanook (M), Saskatoon (S), Kiruna (K), Barrow (B), Cape Chelyuskin (CC), and Cape Schmidt (CS). The fixed coordinate system indicates geographic colatitude and local time, and the mobile one indicates geomagnetic colatitude and longitude. Heavy lines represent the aurora, and arrowheads on the lines indicate the direction of motion of irregularities along the auroral forms. The straight, dashed line near midnight separates the regions of primarily westward and primarily eastward auroral motion at the auroral zone. (After Davis, 1961)

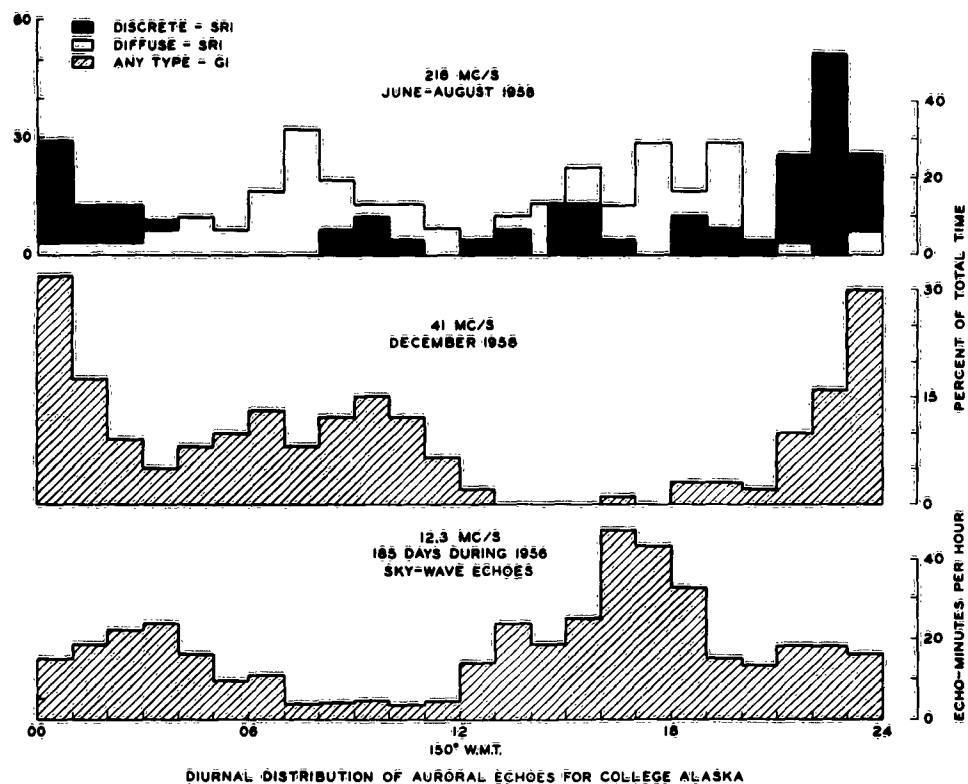


Fig. VII.2

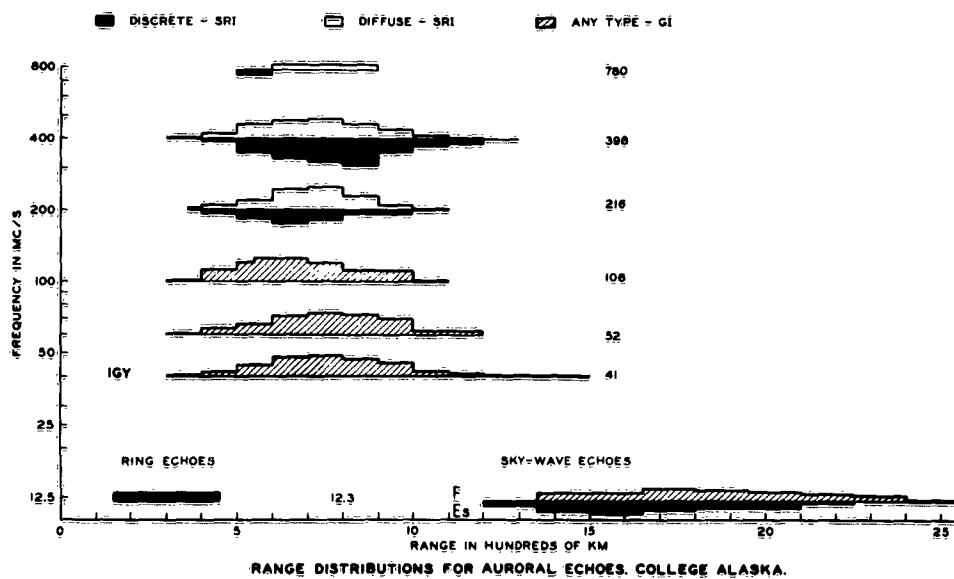


Fig. VII.3

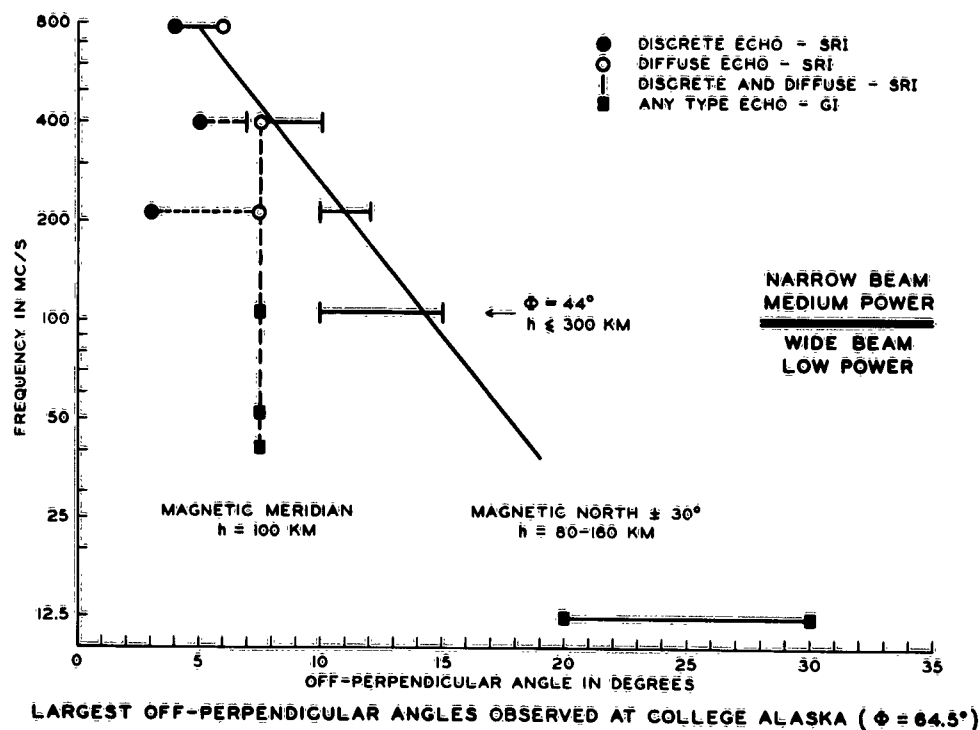


Fig. VII.4

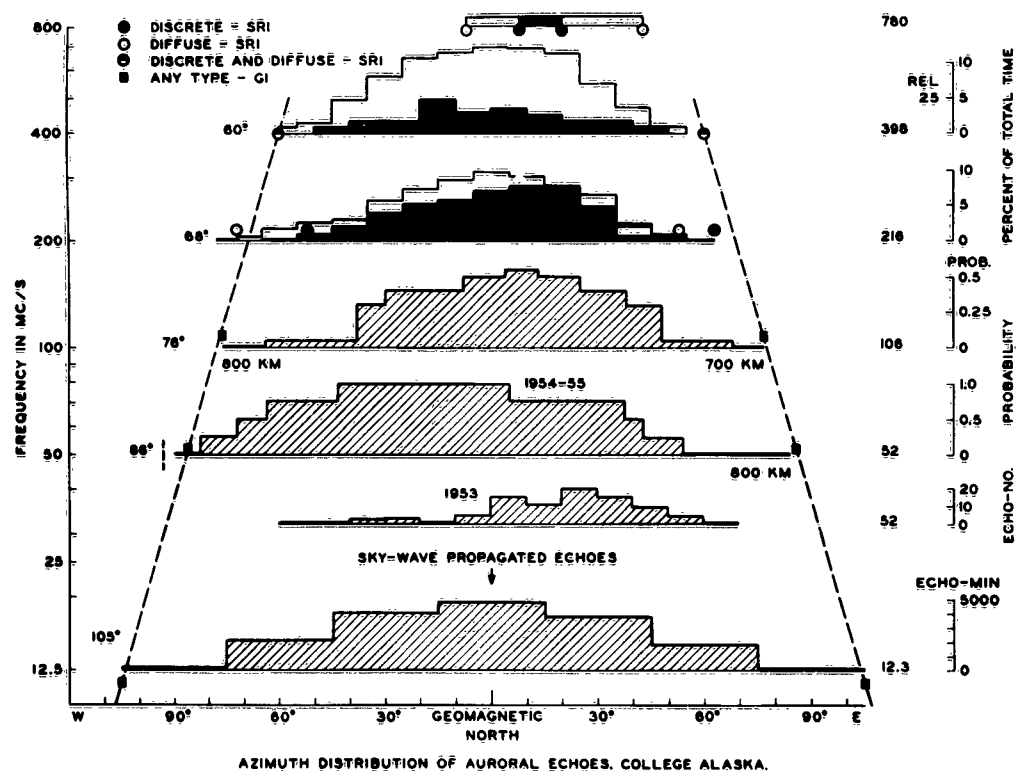


Fig. VII.5

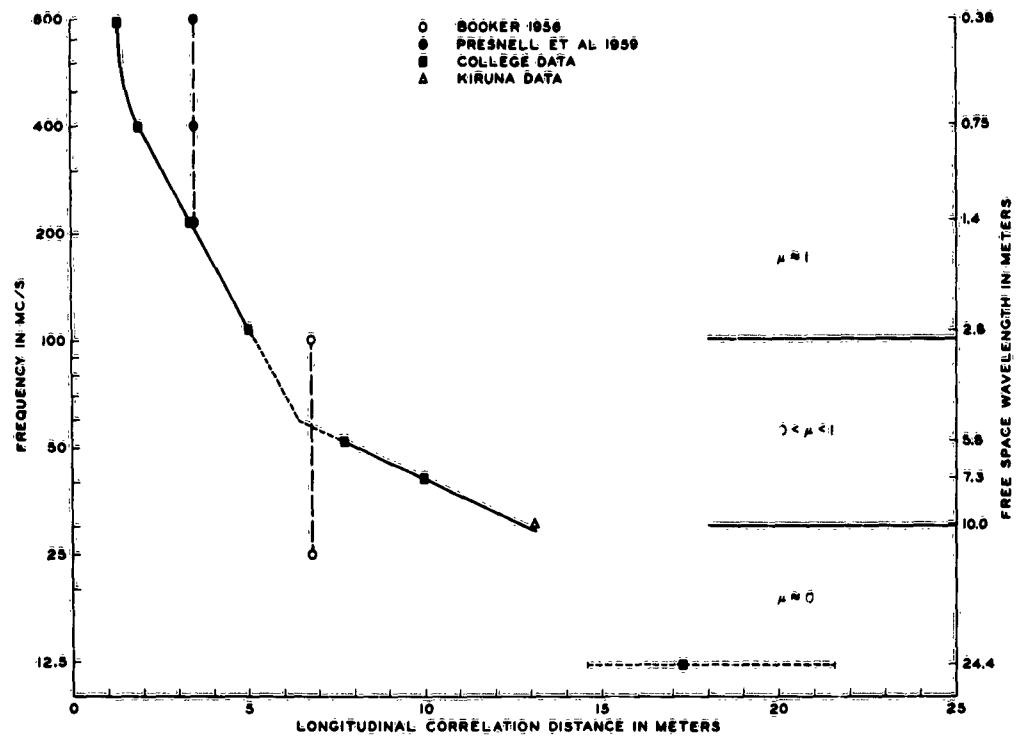


Fig. VII.6

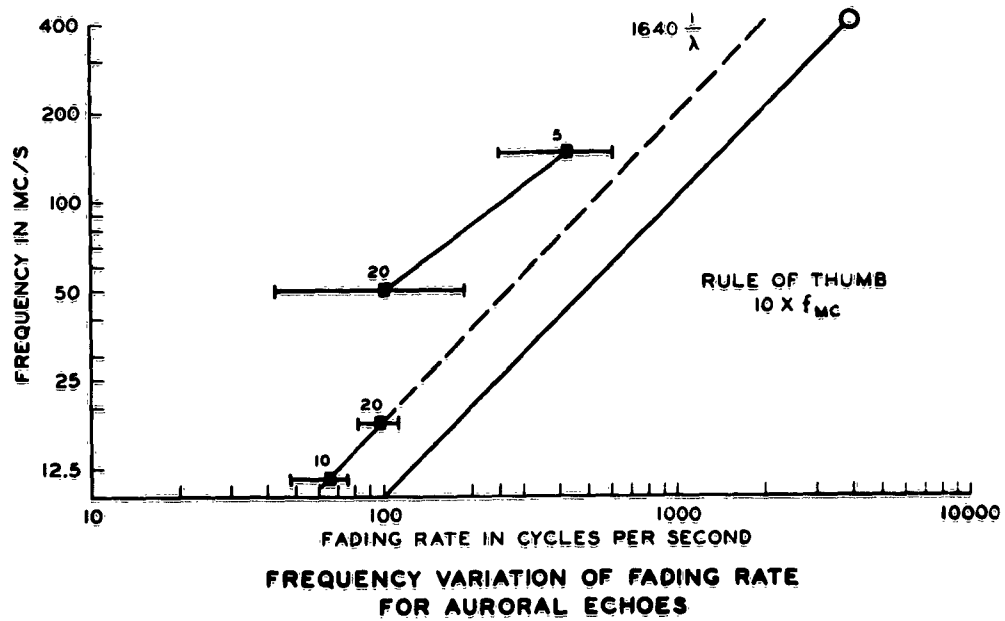


Fig. VII.7

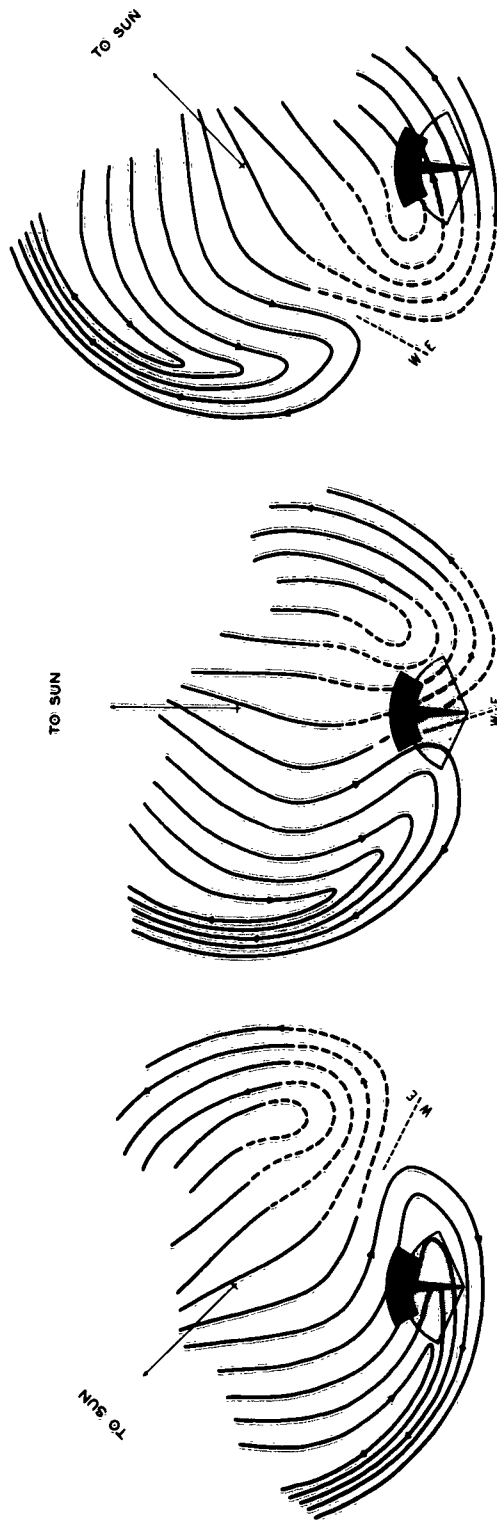


Fig. VII.3 Regions from which Doppler shifted auroral echoes were obtained by Nichols (lightly shaded areas) and by Leadebrand et al (solid black area) relative to the auroral pattern deduced by Davis at times (a) prior to magnetic midnight, (b) near magnetic midnight, and (c) after magnetic midnight.

APPENDIX I
Contents of Previous Reports

(I) Quarterly Progress Reports:

- (1) Quarterly Progress Report Nos. 1-5, 7, 8 (1 June 1956 - 31 August 1957, 1 December 1957 - 31 May 1958) (one Volume). This report contains a brief description of the phase-switch interferometers, and the principal results of the analysis of one year's recordings. The solar time and zenith angle dependence of scintillation amplitude are discussed in detail, and an account is given of some preliminary angular scintillation analysis. An adaptation of Booker's theoretical results to the case of anisotropic irregularities is included.
- (2) Quarterly Progress Report No. 6 (1 September 1957 - 30 November 1957). This report contains a brief description of the phase-sweep interferometer and discusses preliminary results obtained with this equipment. There is an extensive discussion of the long-duration fades of the star signal and their interpretation. Some preliminary analysis of phase-switch data is included, but is greatly extended in the above report.
- (3) Supplementary Progress Report (August 1958). This report contains detailed results of the angular scintillation analysis at 223 Mc/s. Curves showing RMS angular scintillation as a function of index number and the relative probability of occurrence of angular deviations greater than a given amount are included.

- (4) Quarterly Progress Report No. 9 (1 June 1958 - 31 August 1958). Further details of the angular scintillation analysis at 223 Mc/s are included.
- (5) Quarterly Progress Report No. 10 (1 September 1958 - 30 November 1958). This report contains the results of angular scintillation analysis at 456 Mc/s and a brief description of the digitizing equipment designed for use with the phase-sweep interferometer. Samples of power probability distributions obtained with this equipment are included.
- (6) Quarterly Progress Report Nos. 11-12 (1 December 1958 - 31 May 1959) (one volume). This report contains a theoretical treatment of the probability distributions of received power under varying conditions of diffracted wave intensity. A method of relating our $\overline{(\Delta P/P)}$ parameter to the diffracted wave intensity is pointed out.
- (7) Quarterly Progress Report No. 13 (1 June 1959 - 31 August 1959). This report is concerned with the correlation between scintillation activity and other parameters of ionospheric disturbance, including magnetic K-indices, earth potential amplitudes, solar activity and visual auroral activity.

(II) Technical Reports and Notes:

- (1) Technical Report No. 1 (October 1955). This report, prepared as the initial task of the project by C. G. Little, W. M. Rayton and R. B. Roof, was subtitled "Ionospheric Effects at VHF and UHF". It contained a review of existing

knowledge of this field and an extensive bibliography. The review covered a wide scope, including the topics of radar reflections from aurora, absorption, auroral radio noise, ionospheric refraction, radio star scintillation, and radar reflections from meteors and the moon.

- (2) Final Report (Phase I) (February 1959). This report was primarily intended to cover the engineering aspects of the project (Phase I), but the first section was devoted to a general description of the aims of the experiment and of the techniques used. The second and third sections contained respectively descriptions of the field installation and the electronic circuits of the phase-switch interferometer.
- (3) Supplement to Final Report (Phase I) (January 1960). This report was intended to supplement the above report by including the electronic circuitry associated with the phase-sweep interferometers, including the digitizing and data-processing equipment.

(III) Papers Published in the Open Literature and Presented at Scientific Conferences:

- (1) "Review of Ionospheric Effects at VHF and UHF" by C. G. Little, W. M. Rayton and R. B. Roof, Proc. I.R.E., Vol. 44, pp. 992-1018, (August 1956). This paper was substantially identical to Technical Report No. 1 described above.
- (2) "Fluctuations in the Apparent Amplitude and Position of Extraterrestrial Radio Sources as Observed near the Auroral Zone" by J. M. Lansinger, C. G. Little, R. P. Merritt and

E. Stiltner. Paper read at Commission 5 Meeting of URSI, Washington, D. C., May 1957. This paper contained a brief description of the project and its aims, and a preliminary account of results on amplitude and angular scintillation.

- (3) "Observations of the Zenith Angle Dependence of Radio Star Scintillations at Manchester, England and College, Alaska" by C. G. Little. Paper read at Commission 3 Meeting of URSI, Pennsylvania State University, October 1958. This paper is concerned with the very great discrepancies between observed zenith angle dependence of radio star scintillation and the theoretical dependence recently proposed by Booker. An explanation of these discrepancies is given by taking into account the field-alignment of the ionospheric irregularities causing the scintillation and the finite angular dimensions of the radio sources.